2014

The High Frequency Ultrasonic Diagnostic System for Hard and Soft Tissue Specific Assessments in Dentistry

Bartosz Slak
University of Windsor

The High Frequency Ultrasonic Diagnostic System for Hard and Soft Tissue Specific Assessments in Dentistry

By

Bartosz Slak

A Thesis
Submitted to the Faculty of Graduate Studies
Through the Department of Physics
in Partial Fulfillment of the Requirements for
the Degree of Master of Science
at the University of Windsor

Windsor, Ontario, Canada

2014

The High Frequency Ultrasonic Diagnostic System for Hard and Soft Tissue Specific Assessments in Dentistry

by

Bartosz Slak

APPROVED BY:

K. Taylor
Department of Chemistry and Biochemistry

W. Kedzierski
Department of Physics

R. Gr. Maev, Advisor
Department of Physics

27 January 2014

DECLARATION OF CO-AUTHORSHIP / PREVIOUS PUBLICATION

I. Co-Authorship Declaration

I hereby declare that this thesis incorporates material that is result of joint research undertaken in collaboration with A. Daabous, Dr. A Ambroziak, Dr. W. Bednarz, and Dr. E. Strumban under the supervision of professor Roman Gr. Maev. The collaboration is covered in Chapter 3, 4, and 5 of the thesis. In all cases, the key ideas, primary contributions, experimental designs, data analysis and interpretation, were performed by the author, and the contribution of co-authors was primarily through the provision of experimental hardware, samples and advice.

I am aware of the University of Windsor Senate Policy on Authorship and I certify that I have properly acknowledged the contribution of other researchers to my thesis, and have obtained written permission from each of the co-author(s) to include the above material(s) in my thesis.

I certify that, with the above qualification, this thesis, and the research to which it refers, is the product of my own work.

II. Declaration of Previous Publication

This thesis includes materials from 2 original papers that have been previously published/submitted for publication in peer reviewed journals, as follows:

Thesis Chapter	Publication title/full citation	Publication status
Chapter 3,4,5	B. Slak, A. Ambroziak, E. Strumban and R. Gr. Maev, "Enamel thickness measurement with a high frequency ultrasonic transducer-based hand-held probe for potential application in the dental veneer placing procedure," *Acta of Bioengineering and Biomechanics*, vol. 13, no.	*Published*

	1, pp. 65-70, 2011	
Chapter 3,4,5	B. Slak, A. Daabous, W. Bednarz, E. Strumban and R. Gr. Maev, " Ultrasonic assessment of gingival thickness using a high-frequency ultrasonic dental system prototype: A comparison to traditional methods," *Annals of Anatomy*, 2014	*Submitted*

I certify that I have obtained a written permission from the copyright owners to include the above published materials in my thesis. I certify that the above material describes work completed during my registration as graduate student at the University of Windsor.

I declare that, to the best of my knowledge, my thesis does not infringe upon anyone's copyright nor violate any proprietary rights and that any ideas, techniques, quotations, or any other material from the work of other people included in my thesis, published or otherwise, are fully acknowledged in accordance with the standard referencing practices. Furthermore, to the extent that I have included copyrighted material that surpasses the bounds of fair dealing within the meaning of the Canada Copyright Act, I certify that I have obtained a written permission from the copyright owners to include such materials in my thesis.

I declare that this is a true copy of my thesis, including any final revisions, as approved by my thesis committee and the Graduate Studies office, and that this thesis has not been submitted for a higher degree to any other University or Institution.

ABSTRACT

The numerical assessment of dental tissues is essential when selecting a relevant treatment protocol in the field of dentistry. This will have significant ramifications on the restoration quality of dental tissues.

The aim of the research study presented in this thesis was to validate applicability and obtain non-invasively, quantitative data for hard and soft tissue thickness in dental applications. An ultrasonic system was developed and assembled for the purpose of these experiments. Numerous laboratory trials were conducted to validate system performance against traditional and destructive methods of assessment.

Ultrasonic measurements were found to yield similar values to those obtained from invasive methods. Results obtained in these experiments have validated potentials of ultrasound as a supplementary diagnostic tool for dental healthcare.

DEDICATION

I dedicate this thesis to my parents

ACKNOWLEDGEMENTS

During my study at the University of Windsor, I have had an opportunity to work with intelligent and dedicated individuals and I would like to express my appreciation for their support, encouragement and help in my research.

First, I would like to express my sincere thanks to all the members of The Institute for Diagnostic Imaging Research for input in my education and a great study atmosphere. Especially, I would like to thank to my advisor, Dr. Roman Maev, for his support, ideas and guidance during my research. I wish to thank Dr. Emil Strumban, Dr. Fedar Seviaryn, and Dr. Serge Titov for sharing their knowledge and experience.

In addition, I would like to thank Mrs. Sarah Beneteau, Suong Mancini and Sabina Baraoniciu for providing assistance during my study.

TABLE OF CONTENTS

LIST OF TABLES

LIST OF FIGURES

LIST OF APPENDICES

LIST OF ABBREVIATIONS/SYMBOLS

NDE – non-destructive evaluation

DEJ – dentin-enamel junction

MJ – mucogingival junction

SAM – scanning acoustic microscope

CT – computed tomography

CBCT – cone-beam computed tomography

OCT – optical coherent tomography

ALARA – as low as reasonably achievable

HF – high frequency

ADC – analog to digital

UDS – ultrasonic dental system

TOF – time of flight

DSP – digital signal processing

FPGA – field-programmable gate array

$BATiO_3$ – barium titanate

PZT – lead zirconate titanate

PVDF – polyvinylidene fluoride

FWHM – full width at half maximum

DOF – depth of field

GT – gingival thickness

ET – enamel thickness

CHAPTER 1.

INTRODUCTION

Ultrasound is a well known and established technique used in many various fields. The most common use of this technology is in the field of medical diagnostics and in the industry known as Non-Destructive Evaluation (NDE). There are many other popular applications including therapeutics in medicine, industrial cleaning, mixing, chemical process acceleration, and ultrasonic welding. In addition, more general utilizations exist such as distance detection and layer thickness measurements. The main difference between all mentioned applications is the characteristic parameters of the propagated waves through the medium of interest, mainly power and frequency. These two features govern the applicability of ultrasound regarding whether the system is for diagnosis, therapy or other uses.

In the medical field, ultrasound technology can be distinguished by two main applications as mentioned before: therapeutical and diagnostic. Both are highly specialized and differ significantly in requirements for safety and system performance. In therapy, higher intensity waves can interact with the tissue to generate therapeutic heat or damage (for instance lithotripsy). In imaging however, ultrasound has achieved renowned success as a result of its portability and generally low cost in comparison to other available modalities. At the same time it has attained a comparably high resolution as well as a lack of bioeffects.

Ultrasound has been used intensively and has obtained its popularity mostly in obstetrics and gynecology due to its harmlessness. Currently, this technology has become very popular in many fields of medicine.

The main idea about ultrasound for the purpose of diagnosis involves a system which consists of both hardware and software. The hardware is usually represented by a computer module connected to a digitizer with a pulser/receiver circuit and signal conditioning. An electronic pulse controlled from the computer drives the transducer which generates ultrasonic short-time waves (pulse-echo mode). The waves penetrate a targeted object and interact with its interfaces and volumetric structure. Reflected signals are received by the same transducer, amplified, digitized and transferred to the computer for further analysis. Data can be presented in a variety of different modes such as the amplitude mode, also referred to as an A-scan. It is a representation of the amplitude of reflected echoes in the time domain. Conversely, a B-scan representation is a two-dimensional image. The amplitude data from each A-scan is presented as a vector of gray scale pixels alongside positioning information of the transducer (usually linear translation or rotation by a stepper motor or multi-element array). Less popular in medical applications is the M-scan presentation (also known as a time-motion scan). It is a two-dimensional presentation however there is no transducer displacement involved. These recorded A-scans are obtained from the same position as a function of time. There are numerous other presentations available in the ultrasound field, for instance C-scan in the scanning acoustic microscopy or Doppler presentation in fluid velocity measurements.

There is a niche for ultrasonic devices in highly specified, narrow-band applications. Requirements posed by mechanical parameters, geometry and accessibility of objects in most of these cases limit usage of traditional ultrasonic systems and generating an area where much study is required for new developments. All experimental work was conducted on specifically designed phantoms and porcine cadaver samples with cross-sectional views exposed for validation purposes. The measurement results were also compared to dental gold standard techniques commonly used in everyday practice.

1.1. Project Motivation and Background

The motivation for the research performed and described in this thesis is the demand for systems used for non-invasive diagnostics in dentistry. The enamel and gingival thickness cannot be assessed accurately using available modalities due to accessibility and resolution issues. Traditional dental non-invasive diagnostic methods include visual assessment based on the practitioner's experience, non-direct measurements involving a correlation (for instance coronal size to gingival thickness ratio) and gauging with poorly scaled simplistic dental tools. The gap between requirements could be filled by utilizing ultrasound technology. The challenge in the system is to find the trade-off between ultrasonic parameters, depth of wave propagation and resolution to be capable of obtaining expected measurements.

It must also be mentioned, that currently, there is no dental ultrasonic diagnostic device available on the market. However, recent literature shows promising results and prototype developments for this application.

1.2. Dental Anatomy

A typical human adult has 32 teeth, evenly divided in the maxilla and the mandible. Each tooth has a layered structure composed of hard enamel, a bone-like dentin, and a root canal containing nerves and blood vessels. All the teeth are surrounded and supported by a dental periodontium which consists of 3 main components: a gingiva (gums), a periodontal ligament and an alveolar bone [Fig. 1.1].

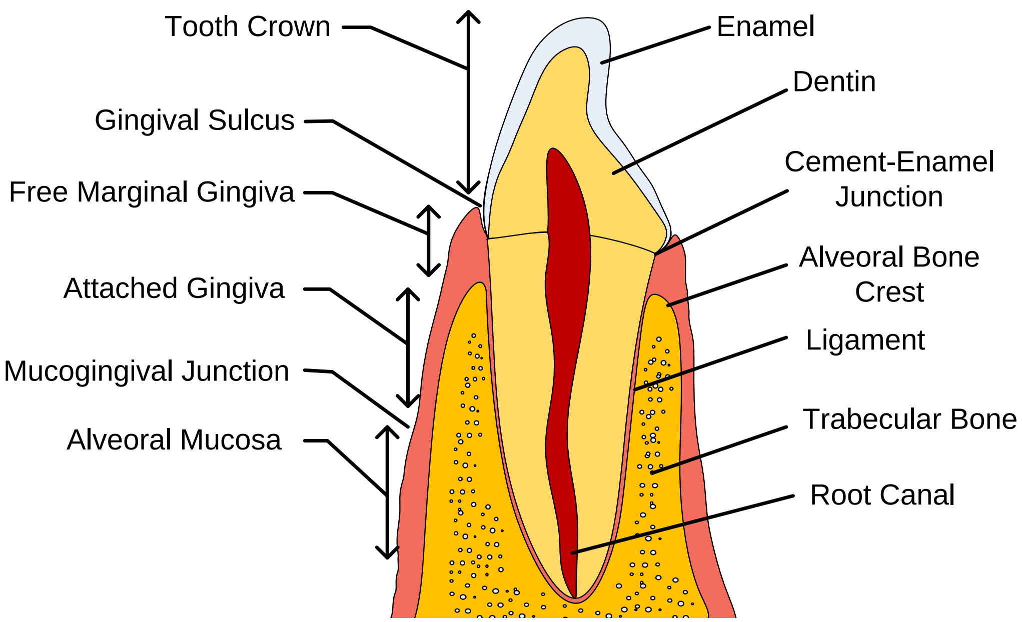

Figure 1.1 The diagram presents a schematic cross-sectional view of a periodontium and a tooth.

In general, a tooth could be divided into a coronal and root piece (embedded in the bone). From the buccal and labial side, a gingival tissue covers the surface of the bone crest. There are 4 anatomical areas on the gingiva surface, starting from the gingival margin, and moving towards an apical direction: first is the free marginal gingiva, which creates a dental pocket (physiological depth should not exceed 3 mm). Next is the attached gingiva; it is a keratinized part of the soft periodontal tissue with increased resistance to possible external injuries as well it stabilizes the gingival margin [1]. The mucogingival junction (MJ) is an important navigational point in a periodontium. Distance between probed pocket depth and MJ is critical and it can represent mucogingival defects. The last element is the alveolar mucosa. It is a membrane located apically to MJ, covering the alveolar process and loosely attached to the bone. Figure 1.2 presents the frontal view of a human periodontium with commonly used navigation points in periodontology.

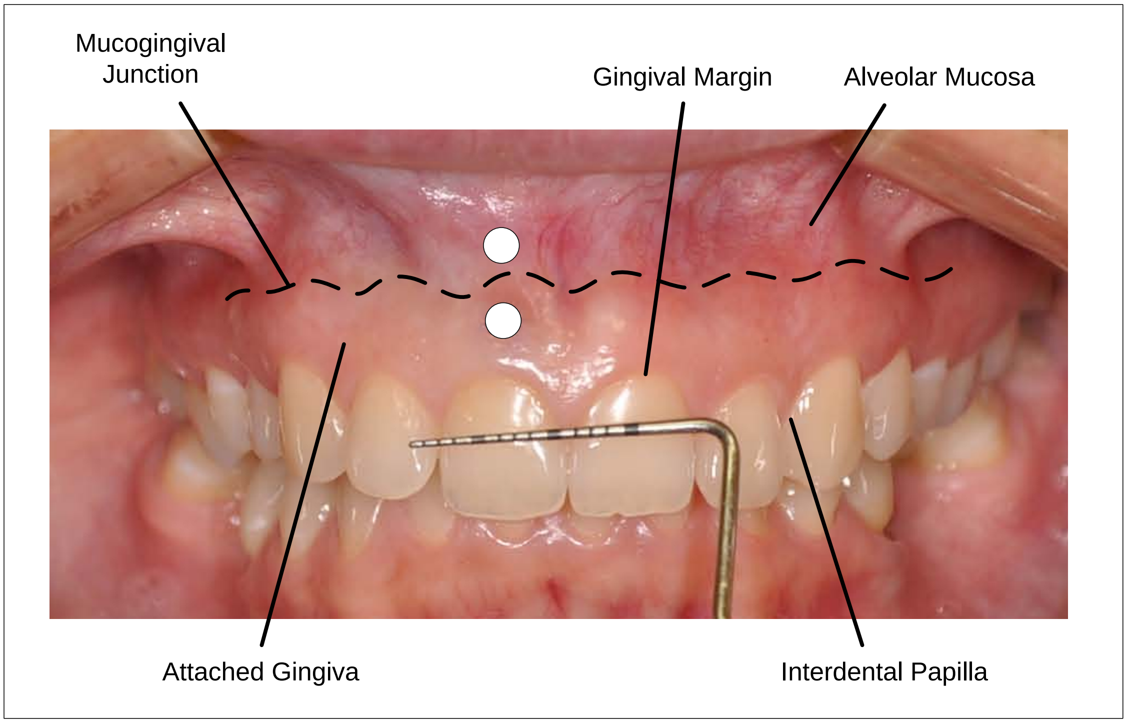

Figure 1.2 The labial view of a human periodontium. Two white spots above #11 tooth (according to FDI World Dental Federation notation) are the proposed measurement points for gingival thickness assessment described in detail in the later chapters.

1.2.1. **Dental Tissues – Structure, Mechanical and Acoustical Properties**

Hard dental tissues are composed from a combination of minerals, proteins and water where the soft parts of the human periodontium mostly consist of water. The enamel layer is considered the hardest tissue in the human organism and its thickness is not uniform over the tooth surface, it is broad at the masticatory surface and becomes narrow towards the apical direction. In most cases, it does not exceed 3 mm in thickness. Internally, enamel has a rod (prism) structure with a diameter of 4-6 μm. It is composed of various apatites: hydroxyapatite, carbonapatite and chlorapatite which are the major prism units [Fig. 1.3]. Inorganic compounds constitute the majority of the enamel mass while the rest is water and proteins. The matrix supports maximum stress from the enamel surface up to the dentin-enamel junction (DEJ) [2].

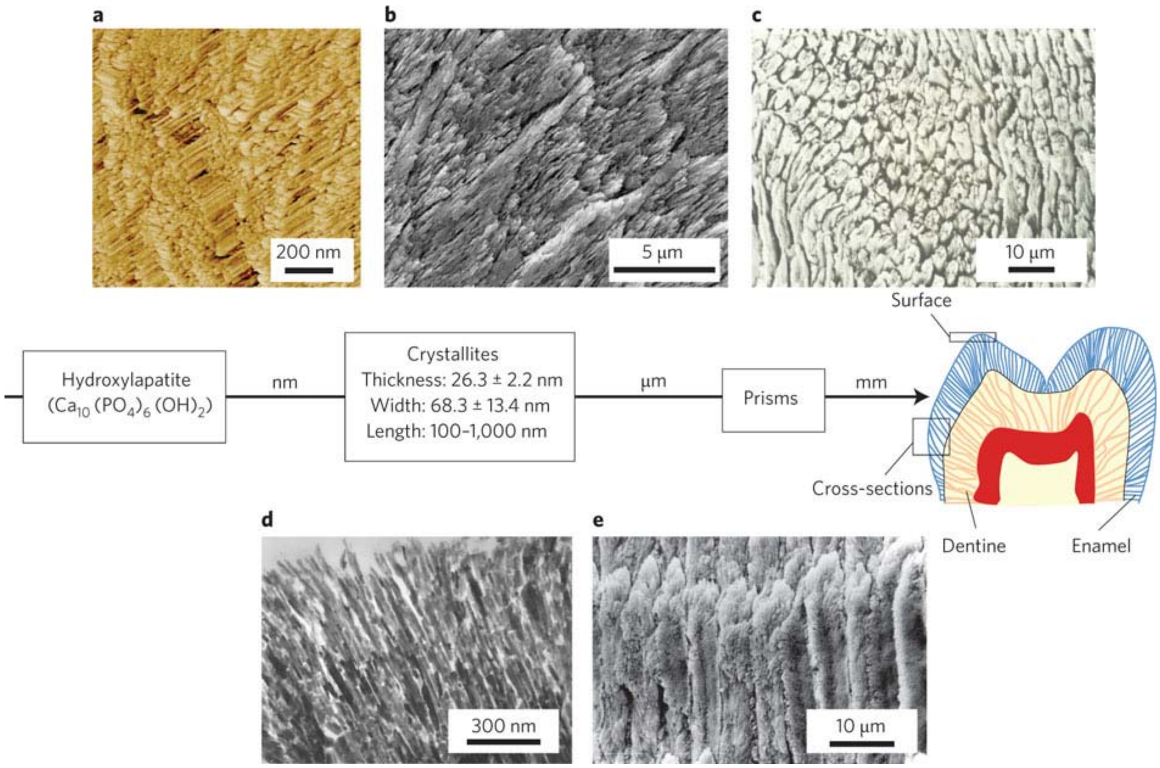

Figure 1.3 The enamel is composed of organized hydroxyapatite crystalities (a, b, d) that are arranged into micrometer-sized prisms (c, e). (a) Atomic force microscope (b) (c) scanning electron microscope images of the enamel surface. (d) Transmission electron microscope image. (e) Image of a cross-section of the enamel [3].

The basic inorganic material of dentin is known to be potassium phosphate (around 70 % of its volume). Similar to the enamel, dentin also contains water and proteins. Dentin has a tubular structure which runs continuously from the DEJ to the pulp chamber in the root. The number of micro tubes ranges from 30000 to 75000 per 1 mm^2 [4], [5].

An important part of the human periodontium is the cementum which acts as a natural protective layer over a dentin. It consists of mineralized connective tissues resembling bone and acts as an anchor to gingival and periodontal fibers. Opposite to cementum, the periodontal ligament has neural and vascular components. The main function of that connective tissue is to join the cementum and alveolar bone. It is also a shock–absorber with various resistance mechanisms providing protection from light as well as greater forces. The last of the crucial elements of periodontium is the alveolar bone. The alveolus (tooth housing) is composed of a thin plate of cortical bone. The rim on the top of the bone is called an alveolar crest (the bone edge). In normal conditions, the distance between the crest and cement-enamel junction should be around 1 to 2 mm and it is a determinant of biological width (distance from gingival margin to alveolar crest) [6]. Mechanical and acoustical properties of chosen components of a human dental periodontium and teeth are listed below [Tab. 1.1]. However, it should be noted that the evidence of anisotropy and inhomogeneity were reported in the literature as well as effect of acoustic dispersion [7], [8]. Moreover, the influence of wear, age, tooth types, storage and measurement conditions on mechanical properties have been analyzed in the present study [9], [10], [11].

Table 1.1 Averaged mechanical and acoustical properties (rough estimation with max error of 20 %) of chosen hard and soft dental tissues [7]- [12].

Tissue	Elastic Modulus $[GPa]$	Poisson's Ratio	Density $[kg/m^3]$	V_L $[m/s]$	Acoustic Impedance $[MRayl]$
Enamel	130	0.33	2970	6250	18.8
Dentine	14.7	0.31	2140	3800	7.6
Bone (cortical)	14.7	0.30	1300	3700	4.8
Cementum	N/A	0.31	2030	3200	6.5
Gingiva (keratinized)	20 MPa	N/A	1060	1540	1.6

1.2.2. History of Ultrasonography in Dentistry

Historically, diagnostic ultrasound technology for dental applications was first attempted in the 1960s. Preliminary research was focused on applying a pulse-echo mode for the examination of the internal tooth structure [13], [14]. At the beginning of the 1970s, the first ultrasonic measurements were applied also to the soft tissue of the human periodontium. Early soft tissue studies lead to more advanced research, which continued into the mid 1980s, and was conducted by scientists in the United States, Germany and Japan [15], [16], [17]. Also another thread of ultrasonic technology in dentistry was emerging at that time - Scanning Acoustic Microscopy (SAM). With high frequency (HF) signals and focused transducers, this method offered the best characterization capabilities. Unfortunately, this technology was not applied in vivo due to setup complexity and initial sample preparation requirements [18], [19]. Tooth material properties, anisotropy and inhomogeneity of different structure layers were the main objectives of studies at that time.

More recent studies, due to advances in computing power and ultrasound technology, have expanded scientists' interest to pathological assessments. Caries detection, erosion monitoring and dental pocket depth measurements were one of the important objectives of studies performed in vitro and in vivo. Moreover, towards the end of the 1990s and during the 2000s, research work was expanded to numerous computer simulations for better understanding of wave propagation in complex dental structures. The knowledge acquired in this way was applied to the dental ultrasonic transducer and device developments.

1.2.3. Recent Advances of Ultrasound in Dentistry

Recent literature from the past decade pertaining to ultrasound technology in dentistry has been studied. Publications for this literature review were distinguished by four groups of applications [Tab. 1.2].

Table 1.2 The recent literature for dental ultrasound – a review.

Application	Literature
Enamel thickness measurements (hard tissue)	Low [20], Hua [21], Bozkurt [22], Huysmans [23], Louwerse [24], Slak [25]
Gingival thickness measurements (soft tissue)	Aydin [26], Muller [27], Bednarz [28], Bednarz [29], Slak [in press]
General ultrasonic dental imaging	Harput [30], Dos Santos [31], Tsiolis [32], Salmon [33], Chifor [34], Hughes [35], Culjat [36], Hughes [37]
General dental research using ultrasound	Maev [10], John [38], [39], Denisova [40], [11], Harput [30], Zheng [41], Bakulin [42],

Starting from the experimental work involving hard dental tissues, most of the studies' focus was on enamel and dentin properties as well as thicknesses. Some of the authors have presented experiments testing possible uses of ultrasound to monitor dental erosion [23], and concluded that it is feasible without initial enamel preparation. However, tests showed that enamel thickness changes of less than 0.3 mm cannot be detected reliably [24]. A commercially available 15 MHz transducer was used in these studies.

Subsequently, abrasive changes in enamel layer, either natural or mechanically applied, were studied [22], [25]. Authors concluded that a nondestructive ultrasonic technique is promising and a system with an 11 MHz transducer provides reliable measurements [22]. Similar results, but obtained with a significantly higher frequency was presented by Maev et al. [25]. The authors stated that a hand-held probe developed for their experiments can be effectively used for enamel thickness measurements before and after the grinding process. In 2009, a study was published where Computed Tomography (CT) images were used as a reference measurement to those obtained by ultrasonic system [21]. A multi-element linear array transducer with 13 MHz central frequency was used with image processing algorithms to generate enhanced B-scan images. Again, the quality of ultrasonic dental assessments was proven experimentally.

Furthermore, similar experimental trials were performed in periodontal applications for assessing soft tissues. In most cases, researchers were focused on masticatory mucosa thickness measurements in different localizations as well as ultrasonic system developments and improvements [26], [27], [28], [29].

New advancements using a variety of commercial systems with a B-scan presentation were broadly discussed in the literature [31], [32], [33], [34]. A critical drawback to this approach is the limited quality and resolution of images presented, which make it difficult for interpretation.

1.3. Other Modalities Currently Used in Dental Imaging and Diagnostics

In general, dental imaging and diagnostic systems are well established and commonly used in daily practice. The majority of them utilize electromagnetic radiation as a physical principle for obtaining images. As part of the scope of this thesis radiography and CT are discussed in detail as commonly used systems. As an example of alternative technology for imaging in dentistry, Optical Coherent Tomography (OCT) was chosen for further discussion [48].

1.3.1. **X-Ray Imaging - Radiography**

The first dental X-ray image was obtained in the U.S. in 1896, just a year after W. Roentgen had discovered “mysterious” radiation [43]. In the dental X-ray system, similar to the traditional body apparatus, the electromagnetic beam is directed onto the tissues of interest. During the propagation its portion interacts with the tissues and results in different intensities due to attenuation. The remaining beam is recorded on an X-ray film localized behind the object. In dentistry, film or a digital detector is usually inserted in the patient’s oral cavity. This technology provides additional information about the bone contour (alveolar crest position in between two teeth), internal anatomy and associated pathologies [44].

A significant limitation of this technique is that it creates projections of 3-dimentional objects on 2-dimentional films, which makes such images difficult to interpret. In addition, highly attenuating dental materials, metal crowns, and even enamel layer limit visibility of the features localized behind restoration or inside the crown. An additional drawback is the ionization of the radiation used in the system. The general radiation exposure principle ALARA (As Low As Reasonably Achievable) should be applied. Furthermore, since the 20th century, two significant advances have been made on dental radiology: panoramic imaging and tomography.

1.3.2. **Cone-Beam Computed Tomography (CBCT)**

The technology of X-ray computed tomography is fairly new in medical diagnostics. The first commercially available unit was created at the beginning of the 1970s. Over the years, the system’s technology was improved and successive generations were released to the market. Generally in these systems the targeted area is exposed to a fan-shaped or flat sliced radiation beam as the unit makes multiple revolutions around the patient to acquire data for further reconstruction. Conversely, in the CBCT unit, the X-ray is divergent creating a cone-shaped beam which requires just a single scan. Therefore, this method is lower in absorbed dose and exposure time than traditional CT units. Moreover, the CBCT system can generate 3-dimensional data of the craniofacial region and allow reconstructing cross-sectional views [Fig. 1.3] [45].

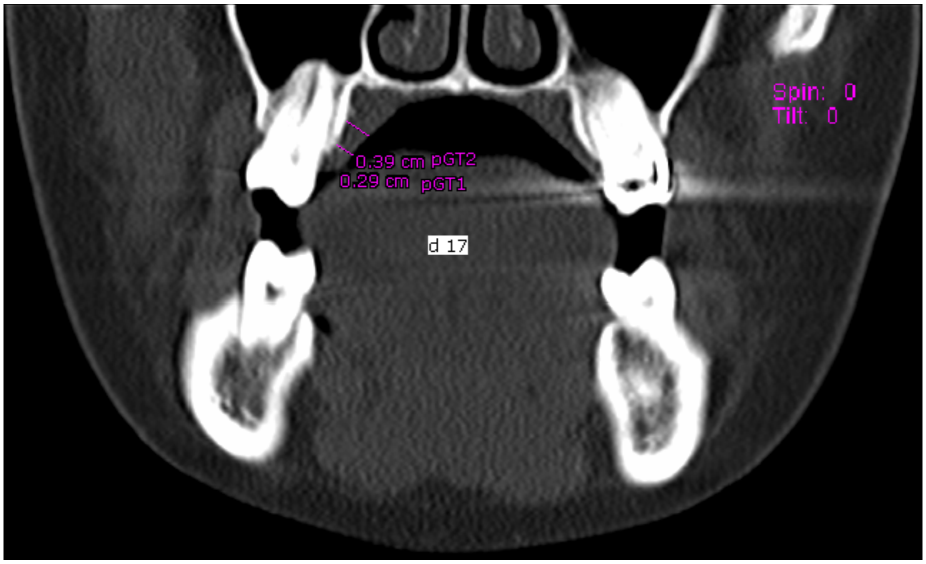

Figure 1.4 A CBCT cross-sectional image with hard palate, soft tissue thickness measurement results. Image contrast was exaggerated, which partially allows imaging of soft tissues (*Courtesy of Dr. Bednarz*).

1.3.3. **Optical Coherent Tomography (OCT)**

The OCT system was initially described in 1991 and in experimental dental imaging had been initiated by 1998. The OCT unit is an interferometer-based optical system with a low coherence length broadband light source. The system demonstrates excellent axial and lateral resolution for dental imaging and detection of pathological changes, although the penetration depth is limited. This is one of the factors preventing popularization of dental OCT. Another factor is the insufficient scanning range (usually a few millimeters). New systems with improved light sources and probes are still under development to overcome these and other limitations [46].

1.4. Requirements and Specifications for Dental Ultrasonic System

The main idea behind the experimental research design for this study was to mimic actual conditions in the dental environment. This assumption generated a list of requirements for the experimental setup. It helped to set criteria for the wave beam parameters, the unit and the probe design as well as the time constraints for acquiring data, performing calculations and managing obtained information.

An important requirement was the enhancement of a system's resolution due to the high velocities of sound in hard dental tissues and relatively small anatomical objects of interest. As a result, it has been decided to use a single element transducer with a spherically shaped emitting surface to increase lateral resolution, in comparison to traditional flat elements. Moreover, to enhance the axial resolution, a 50 MHz central frequency was proposed. This frequency range was chosen based on literature study, initial calculations and laboratory trials. There are other beam parameters that require optimization to achieve legitimate results and they will be discussed in later chapters, mainly: aperture, localization of the focal point and depth-of-field.

Regarding the design of the system, the main requirement of the system's probe was to create it with the size and shape such that the probe will be similar to currently used dental handpieces, for instance a dental rotor or turbine. Reasons for these specifications are to allow access to all potential measurement areas for both teeth and gingiva, especially on the buccal and lingual side.

Lastly, further requirements for the hardware (system's unit) were mostly related to the size, portability and the communication interface. Due to the embedded micro computer and the integrated ultrasonic board, the system's unit was comparable in size to currently available computer tablets. A resistive touch-screen, foot controller and beeping signals were proposed to limit cross infections and simplified communication with the device. Also, an intuitive interface with automatic signal detection algorithms is also required to keep measurement times short.

Overall, the system should be compact, easy to operate, fast to boot-up and inexpensive (at this level of development, the system is not equipped with scanning elements or multi-element arrays to obtain images, due to an effort to reduce cost). The aim of this project was to experimentally prove whether HF ultrasound technology is applicable in clinical dentistry and at the same time develop a prototype of an ultrasonic system for dental assessments as a complementary tool to other widely used dental diagnostic modalities.

1.5. Summary

This introduction provided a general outline to ultrasound in the medical field along with a description of ultrasonic systems and a set of system requirements for the potential application in dentistry. The proposed research is mostly motivated by the demand for non-invasive diagnostic devices as well as a lack of specialized measurement tools for dental application.

The system proposed can perform measurements, which could allow practitioners to choose better protocols and predict ultimate surgical outcomes with higher accuracy. The HF ultrasound diagnostic technology then seems to be a perfect solution in modern dentistry, especially in the area of esthetic procedures, mucogingival surgery and implantology.

The most popular dental diagnostic modalities were briefly described in this chapter and the short summary below [Tab. 1.3] presents the main advantages and disadvantages of the systems including current techniques, uncommonly used techniques and ones still under development.

Table 1.3 Comparison of different imaging modalities applied to the field of dentistry.

Diagnostic Methods	Advantages	Disadvantages
Traditional X-ray	Low cost Broad measurements	3D object projected on 2D image Limited resolution Hidden objects
CBCT	3D image reconstruction	No real time image Source of ionizing radiation
OCT	High resolution 3D image reconstruction possible	Limited depth penetration Expensive system
Ultrasound	Real-time image Low cost Non-invasive	Trade-off between resolution and depth propagation
Digital Camera/ Microscopy	Low cost	Only surface information
Laser fluorescence spectroscopy	Real – time detection	No image Lack of consistency
Traditional Periodontal Probe	Low cost	Inaccurate, subjective, no image, not consistent, low resolution, invasive

For over a decade, the development of an ultrasonic technique to measure oral tissue thickness has been underway. Ultrasound technology has the potential to offer a painless, accurate and quicker method of obtaining results compared to traditional methods. However, until recent years, a lack of technological progress with regards to both electronics and HF transducers had limited its ability to achieve reliable measurements. Moreover, the majority of research performed with ultrasound has used devices originally designed for applications other than dentistry [47], [48], [49].

CHAPTER 2.

PHYSICS OF ULTRASOUND PROPAGATION

Ultrasound is indentified to be a mechanical disturbance propagating as a wave at a frequency above the level of audibility. A propagating medium is required, which must offer inertia (related to medium density) and elasticity.

In this chapter, a theoretical introduction of acoustical wave propagation in fluids and solids is presented. The behavior of an ultrasonic wave traveling through material interfaces is shown (for example a fluid-solid interface). The equations for transmission and reflection coefficients are derived along with calculated angular dependence for an oblique incidence according to material properties involved in the experimental study (enamel and gingival tissues). Further, basic ultrasonic properties of tissues are discussed, mainly: absorption and wave scattering, which are known generally as a sound attenuation.

The concept presented for the physics of ultrasound propagation is necessary to understand waves generated by a transducer, and to evaluate its required parameters. Many of the physical principles were purposely abbreviated, due to objectives of this thesis; descriptions that are more detailed are available in textbooks and articles referred in this chapter.

2.1. Introduction

An audio spectrum, which represents a full frequency bandwidth, has various areas with common frequency ranges, which are applied in different fields of ultrasonic technology [Fig. 2.1].

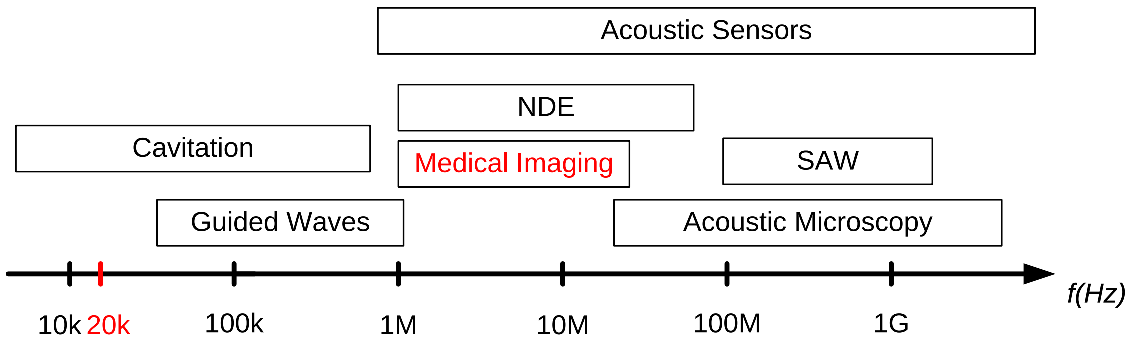

Figure 2.1 Common frequency ranges for various ultrasound applications.

The standard human receptor response function covers frequencies in the range of around 20 Hz to 20 kHz, where the band limits depend on health condition and age. The standard human bandwidth is a small portion of the audio full spectrum and characterizes all possible sounds heard. Ultrasound is defined as the audio spectrum above 20 kHz and it continues up to values of around 1 GHz and higher, where its conventionally called the hypersonic regime. Most of the medical applications are in the range of kilohertz for therapeutic, and megahertz for diagnostic purposes. The physics phenomena, for instance the diffraction and dispersion, occur for the entire acoustic spectrum, but their relative importance changes with frequency.

The two main features of ultrasonic waves which make this technology unique, extremely popular and useful is the speed of propagation and the ability to easily penetrate opaque materials [50].

2.1.1. **Ultrasound Wave Propagation [50], [51]**

Prior to studying propagation of ultrasound through interfaces, a basic introduction to wave propagation must be given. The discussion starts from simple assumptions and application of Gauss' theorem on a 3-dimensional fluid volume object and is followed by an introduction to a tensor-based derivation of a wave equation for solids in the Cartesian coordinate system using the concept of tensors (stress and strain).

2.1.2. **Wave Equation for a Fluid**

The principle of conservation of momentum shows how an ideal compressible fluid, of an arbitrary volume V, can be described by the differential equation:

$$-\bar{\nabla}p(\bar{x},t) + \bar{f}(\bar{x},t) = \rho\bar{a}(\bar{x},t) \tag{2.1}$$

Where $p(\bar{x},t)$ is the pressure in any point $\bar{x}$ and time t in volume V, $\bar{f}$ and $\bar{a}$ are the body force (force/unit volume) and acceleration of the fluid, respectively, and ρ is the fluid density. After introducing the definition of acceleration, and the assumption of density being the same in the volume V, equation 2.1 turns to:

$$-\bar{\nabla}p + \bar{f} = \rho_0\frac{\partial^2\bar{u}}{\partial t^2} \tag{2.2}$$

The variable $\bar{u}$ in this equation is the displacement vector (the equation is presented in an abbreviated form for simplicity, without showing dependency of the field variables). The pressure is then shown to be proportional to the divergence of the displacement (a constitutive equation):

$$p = -\lambda\bar{\nabla}\cdot\bar{u} \tag{2.3}$$

Where λ is the bulk modulus for a fluid (proportionality constant) which it is true for an ideal compressible fluid.

The dilatation term $\bar{\nabla}\cdot\bar{u}$ in equation 2.3 is the relative change in the elementary volume while the negative sign means that the volume decreases when positive pressure is applied. In terms of speed of sound in the fluid ($c = \sqrt{\lambda/\rho_0}$), and using the dependences presented, we can obtain the three-dimensional inhomogeneous wave equation for pressure in the form:

$$\nabla^2 p - \frac{1}{c^2}\frac{\partial^2 p}{\partial t^2} + f = 0 \tag{2.4}$$

The equation could be rewritten, assuming a disturbance in the fluid varying in only one spatial dimension x, and neglecting the scalar body force term:

$$\frac{\partial^2 p}{\partial x^2} - \frac{1}{c^2}\frac{\partial^2 p}{\partial t^2} = 0 \tag{2.5}$$

The general solution for the wave equation is in the form:

$$p = f\left(t - \frac{x}{c}\right) + g\left(t + \frac{x}{c}\right) \tag{2.6}$$

Where f and g are arbitrary functions and c is the speed of the wave in the fluid. After applying the Fourier transform and inverse Fourier transform, it can be shown that an arbitrary planar wave traveling in $+x$ direction is a harmonic wave of the form:

$$p = Ae^{ik(x-ct)} \tag{2.7}$$

Where $k = w/c$ is called the wave number ($w = 2\pi f$).

2.1.3. **Wave Equation for a Solid**

Similarly, as with the fluid, the principle of conservation of momentum and the Gauss integral transformation drives to obtain the so-called Cauchy equation - a differential equation which can be expressed in terms of Cartesian components with a particle displacement u:

$$\frac{\partial \sigma_{ij}}{\partial x_i} + f = \rho \frac{\partial^2 u_j}{\partial t^2} \tag{2.8}$$

Where σ_{ij} is the stress tensor of the second rank, ρ is the density, f stands for the body forces (such as gravity are negligible in the normal environments) and $i, j = 1, 2, 3$. Symmetry of the stress and strain tensor expressed using particle displacement is depicted by:

$$\varepsilon_{ij} = \frac{1}{2}\left(\frac{\partial u_i}{\partial x_j} + \frac{\partial u_j}{\partial x_i}\right) \tag{2.9}$$

In the above equation it was assumed that the displacement gradient was small (quadratic terms ignored). The stress-strain constitutive equation (generalized Hook's law) can be shown in the form:

$$\sigma_{ij} = C_{ijkl}\varepsilon_{ij} \tag{2.10}$$

Where C_{ijkl} is a fourth-order tensor of elastic constants (elastic stiffness tensor). In general, the statement is valid for the amplitudes of ultrasonic waves below the limit of linearity. Since both stress and strain tensors are symmetric, the symmetry is also reflected in the stiffness tensor which effects in reduction of independent constants from 81 to 36 and hence Hook's law could be presented with the simplified notation:

$$\sigma_i = C_{ij}\varepsilon_j \tag{2.11}$$

$$i, j = 1, \ldots, 6 \tag{2.12}$$

For isotropic solids, additional axes of symmetry will result in further reductions. The stress-strain equation, in matrix form (so-called engineering notation) will take the form:

$$\begin{bmatrix}\sigma_1\\ \sigma_2\\ \sigma_3\\ \sigma_4\\ \sigma_5\\ \sigma_6\end{bmatrix} = \begin{bmatrix} c_{11} & c_{12} & c_{12} & 0 & 0 & 0\\ c_{12} & c_{11} & c_{12} & 0 & 0 & 0\\ c_{12} & c_{12} & c_{11} & 0 & 0 & 0\\ 0 & 0 & 0 & c_{44} & 0 & 0\\ 0 & 0 & 0 & 0 & c_{44} & 0\\ 0 & 0 & 0 & 0 & 0 & c_{44}\end{bmatrix}\begin{bmatrix}\varepsilon_1\\ \varepsilon_2\\ \varepsilon_3\\ \varepsilon_4\\ \varepsilon_5\\ \varepsilon_6\end{bmatrix} \tag{2.13}$$

$$c_{44} = \frac{1}{2}(c_{11} - c_{12}) \tag{2.14}$$

Introducing Lam*é* constants $\lambda = c_{11} - 2c_{44}$ and $\mu = c_{44}$, the matrix representation can be rewritten in a more condensed form:

$$\sigma_{ij} = \lambda\varepsilon_{kk}\delta_{ij} + 2\mu\varepsilon_{ij} \tag{2.15}$$

Where ε_{kk} is the dilatation (change in volume per unit volume). When placing the constitutive equation [Eq. 2.3] into the equation of motion and neglecting body forces, it is possible to obtain Navier's equations for the displacement, which has the final representation:

$$\mu\frac{\partial^2 u_i}{\partial x_j^2} + (\lambda + \mu)\frac{\partial^2 u_j}{\partial x_j x_i} = \rho\frac{\partial^2 u_i}{\partial t^2} \tag{2.16}$$

An assumption was made about the solid body to be homogenous, which affects independency of Lamé constants according to the position. Equation 2.16 could be expressed in a vector notation:

$$\mu\nabla^2\bar{u} + (\lambda + \mu)\,\nabla(\nabla\cdot\bar{u}) = \rho\frac{\partial^2\bar{u}}{\partial t^2} \tag{2.17}$$

The presented equation governs the behavior of wave propagation in an elastic solid. There are various ways of showing the equation and different methods for decoupling longitudinal and transverse modes involving Helmholtz identity. The decomposition process effects in separating into independent equations which are shown:

$$(\lambda + 2\mu)\, \nabla^2 \bar{u}_l = \rho \frac{\partial^2 \bar{u}_l}{\partial t^2} \quad (2.18)$$

$$\mu \nabla^2 \bar{u}_s = \rho \frac{\partial^2 \bar{u}_s}{\partial t^2} \quad (2.19)$$

$$\nabla^2 \bar{u}_l = \frac{1}{c_l^2} \frac{\partial^2 \bar{u}_l}{\partial t^2} \quad (2.20)$$

$$\nabla^2 \bar{u}_s = \frac{1}{c_s^2} \frac{\partial^2 \bar{u}_s}{\partial t^2} \quad (2.21)$$

Where c_l and c_s stand for longitudinal and shear wave velocity, respectively:

$$c_l = \sqrt{(\lambda + 2\mu)/\rho} \quad (2.22)$$

$$c_s = \sqrt{\mu/\rho} \quad (2.23)$$

2.2. Reflection and Refraction of Waves at Interfaces

Any operation performed using the ultrasound pulse-echo technique involves wave propagation through an interface between different materials. Due to the difference in acoustic properties, partial transmissions and reflections at the interface exist. There is a number of standard cases of this phenomena described in the literature [50]. For the scope of this thesis, the fluid-solid interface will be discussed in more detail. Some simplifications to the system were made; a plane wave was assumed to go through an interface between two semi-infinite media.

2.2.1. **Fluid – Solid Interface**

For the simple case [Fig. 2.2], where the plane wave approaches the interface at a normal incidence, there is no mode conversion so a perfect interface is assumed. Applying boundary conditions for the pressure and the velocity, the transmission and reflection coefficients could be calculated and presented in the form:

$$T_p = \frac{p_t}{p_i} = \frac{2Z_2}{Z_1 + Z_2} \tag{2.24}$$

$$R_p = \frac{p_r}{p_i} = \frac{Z_2 - Z_1}{Z_1 + Z_2} \tag{2.25}$$

$$R_p + 1 = T_p \tag{2.26}$$

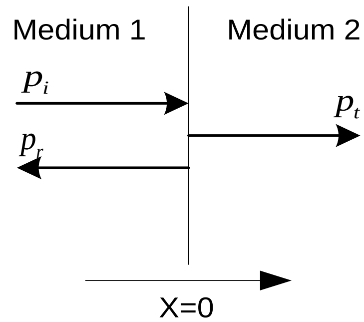

Figure 2.2 The diagram of a normal incidence wave approaching an interface.

Where Z_1 and Z_2 stand for, acoustic impedance in medium 1 and 2, respectively. In general, the characteristic acoustic impedance could be approximated to $Z_m = \rho_m C_m$ (ρ_m- density, c_m- longitudinal velocity in specific medium m), for a spherical wave far from the source. A different set of coefficients must be calculated to identify how energy is partitioned between reflected and transmitted waves. For the case where the wave front is normal to the direction of the propagation, intensity is defined as:

$$I = \frac{p^2}{2Z} \tag{2.27}$$

This effects the coefficients to be in the form:

$$T_I = \frac{Z_1}{Z_2}\, T_p^2 \tag{2.28}$$

$$R_I = R_p^2 \tag{2.29}$$

$$R_I + T_I = 1 \tag{2.30}$$

From this, it can be verified that the conservation of energy is satisfied.

A more complicated case [Fig. 2.3] involves an oblique incidence wave, where a mode conversion occurs. In a solid medium, which supports shear stress, the longitudinal and shear waves will propagate affecting the transmission coefficient for each wave. The system boundary conditions (continuity of normal velocity and stress, and zero tangential stress due to neglected fluid viscosity) allow the solutions for the intensity coefficients to be expressed in the form:

$$T_I^L = \frac{\rho_2 tan\theta}{\rho_1 tan\theta_L}\left|\left(\frac{\rho_1}{\rho_2}\right)\frac{2Z_L cos2\theta_s}{Z_L cos^2 2\theta_s + Z_S sin^2 2\theta_s + Z_1}\right|^2 \tag{2.31}$$

$$T_I^S = \frac{\rho_2 tan\theta}{\rho_1 tan\theta_s}\left|-\left(\frac{\rho_1}{\rho_2}\right)\frac{2Z_S sin2\theta_s}{Z_L cos^2 2\theta_s + Z_S sin^2 2\theta_s + Z_1}\right|^2 \tag{2.32}$$

$$R_I = \left|\frac{Z_L cos^2 2\theta_s + Z_S sin^2 2\theta_s - Z_1}{Z_L cos^2 2\theta_s + Z_S sin^2 2\theta_s + Z_1}\right|^2 \tag{2.33}$$

where

$$Z_1 = \frac{\rho_1 C_1}{cos\theta_i}, \qquad Z_L = \frac{\rho_2 C_{2L}}{cos\theta_L}, \qquad Z_s = \frac{\rho_2 C_{2S}}{cos\theta_S} \tag{2.34}$$

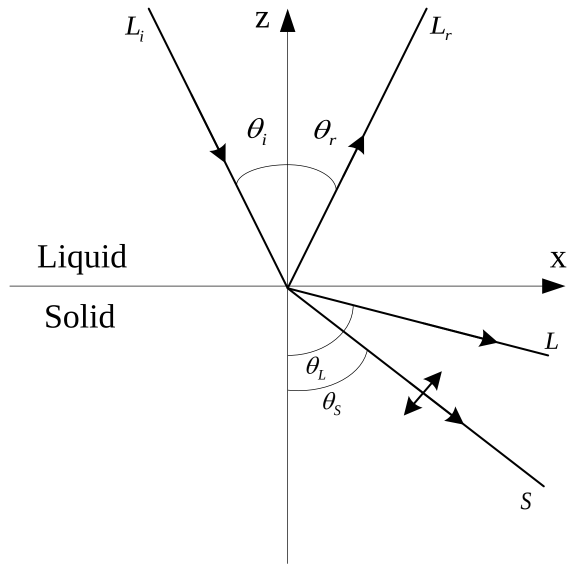

Figure 2.3 The acoustic ray diagram shows a transmission and reflection at a liquid-solid interface with an oblique incidence.

The set of equations [Eq. 2.31-2.34] was used to plot energy to incident angle dependences [Fig. 2.3] (the code is available in the Appendix A). The energy coefficients at the water/enamel and water/gingival interfaces were calculated based on mechanical properties provided in the first chapter, such as the speed of sound and density, and were plotted as a function of an incidence angle [50], [51].

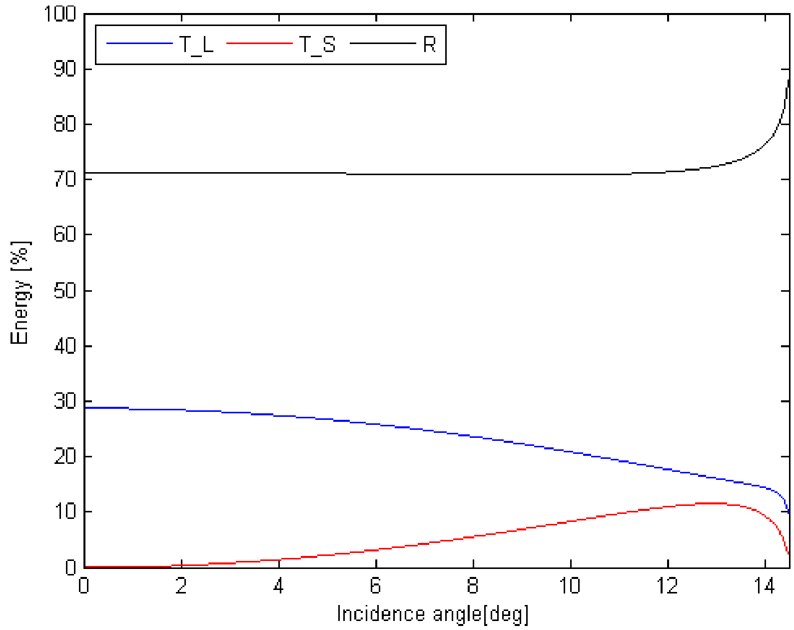

Figure 2.4 The energy level to incidence angle reflection and transmission coefficients for water/enamel interface.

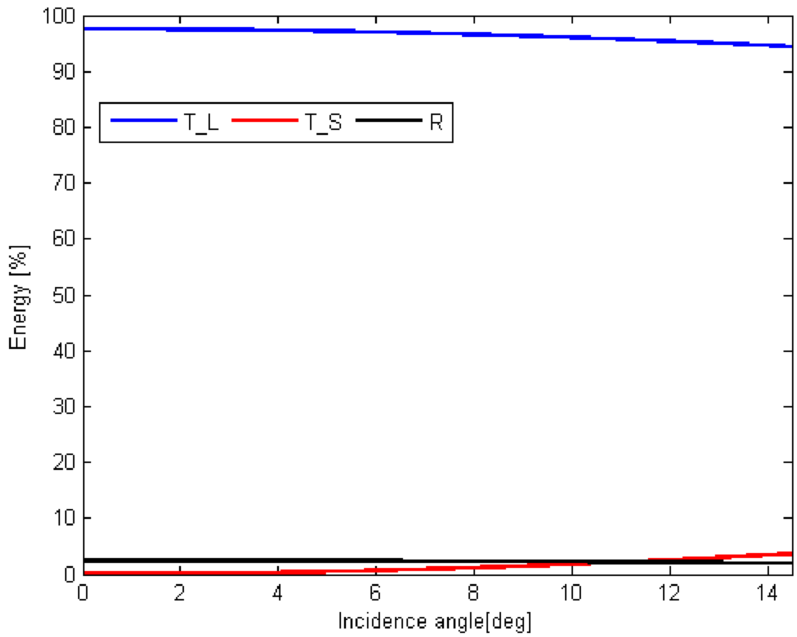

Figure 2.5 The energy level to incidence angle reflection and transmission coefficients for water/gingiva interface.

2.3. Sound Attenuation

The total ultrasonic energy lost during wave propagation in biological tissues is due to two processes: absorption and scattering. Absorption is the transformation of acoustical energy to heat. The scattering effect occurs when the medium re-radiates acoustic waves with different properties than incident waves. The sum of these two processes responsible for the loss of energy is called the attenuation. As an example, scattering for soft tissues accounts for around 2 to 10 %, which means the attenuation effect is caused mainly by absorption.

In general, attenuation reduces the ultrasonic wave pressure, and for a simplified case, when the plane wave travels through a flat tissue slab of thickness d, the relationship between initial pressure and final pressure amplitude of the wave could be presented in the form:

$$p_d(d,f) = p_0(f)e^{-\alpha(f)d} \qquad (2.35)$$

Where p_d and p_0 are the amplitudes of the wave at the distance d and 0, respectively. In case of the pulse-echo technique, and a perfectly reflecting surface, the attenuation coefficient could be written using a power function [$\alpha(f) = \alpha_0 f^n$], to take into consideration a broadband pulse spectrum. Assuming a linearity of attenuation coefficient to the frequency (n=1), the attenuation coefficient could be expressed in the form:

$$\alpha_0 = \frac{1}{2df}\ln\frac{p_0}{p_d} \qquad (2.36)$$

The unit for the ratio value is given in Neper (Np), so units for α_0 are $Np/(cm\ MHz)$. However, the more conventional units for attenuation coefficient are $dB/(cm\ MHz)$. The conversion ratio is $20\log_{10}(e) = 8.6859$, so α_0 has to be multiplied by this factor to get values in decibels [52], [53].

2.4. The Concept of Ultrasonic Transducer Radiation

An ultrasonic transducer is used as a transmitter and a receiver in pulse-echo mode. In the immersion arrangement (water-coupled system, which is also the case of the experimental setup), it radiates a sound beam into a fluid. Then, the beam crosses a boundary between the coupling medium and the object to be diagnosed.

In general, a few assumptions are made to simplify the transducer model and the calculations of the pressure distribution. Usually, a planar piston transducer is assumed (half-spaced, planar surface with zero velocity in z-direction, except over a finite region of a given area). The pressure wave field of the transducer can be considered to arise from a superposition of the elementary point source (spherical waves) on the front face of the transducer. An explicit equation, describing the radiated pressure is called the Rayleigh-Sommerfeld integral (it specifies the field for a plane piston model).

The transducer, proposed for the experimental work of this thesis, produces a non-planar wave front, by means of a spherically curved piezomaterial. In 1945, O'Neil developed a model, based on the Rayleigh-Sommerfeld theory involving radial velocity acting on a spherical surface of a given diameter, surrounded by an infinite plane baffle [54]. The integration over a planar surface is replaced by the integration over the spherical source region. It has been shown that the model is a good approximation especially at higher signal frequencies and not tightly focused elements [51] (radius of curvature is large compared to the wavelength [55]).

There are many commercial and open-source software available, allowing simulations of acoustic fields (solving mentioned integrals with a set of necessary parameters). Usually, integrations are substituted by summations over a finite number of source points and the approximated field is calculated. A common way of presenting these results is a graph of pressure distributions along the acoustic axis and in the plane of the focal point.

2.5. Summary

In summary, a short introduction to ultrasonic wave propagation was given. The governing equations for a fluid and elastic solid medium were also derived. Energy reflections and transmissions for materials involved in the experimental study were calculated and plotted against an angle of incidence. Finally, the concept of tissue attenuation was discussed and a short introduction to the radiation theory was given in order to support the transducer's design.

CHAPTER 3.

THE ULTRASONIC DENTAL SYSTEM (UDS)

The UDS includes several interfaced standard medical apparatus blocks as well as complex ultrasonic elements [Fig. 3.1]. The two important components of the proposed system is the probe with a transducer and an ultrasonic PC board.

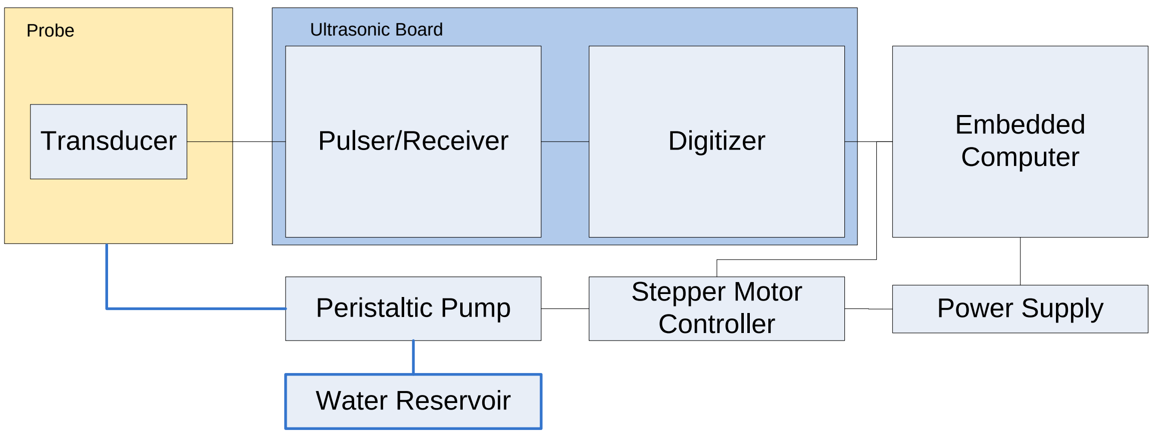

Figure 3.1 Simplified schematic diagram of the ultrasonic dental system component blocks.

The UDS is equipped with a water coupling delay line block operated by a peristaltic pump and controlled from the software. The overall device is managed from a computer built into the main unit. The operating system coordinates data transfer, inputs and outputs information and sets initial parameters.

In this chapter, the theoretical characterization of each component is given along with the design and prototype details. The presented system was assembled, tested using ultrasonic phantoms and used in the research work conducted for the purpose of this thesis.

3.1. The Ultrasonic System Behavior. Pulse – Echo Mode

The pulse-echo mode is the most popular ultrasonic method used in the medical field. The main advantage of it is that it utilizes one transducer for sending and receiving purposes. This method was applied to obtain all ultrasonic measurements in the study presented in this thesis.

As an example, assume that the wave propagates through the water, which acts as the coupling medium, until it strikes an object (assume the object to be a 1 mm layer of polyurethane over a laboratory glass slide). Due to the mismatch of acoustic impedances at the interface, part of the pulse is reflected back to the transducer as an echo. The unreflected wave of the incident pulse continues to propagate through the object until it comes in contact with the next interface. At this second interface, another echo is created, which returns to the transducer and appears as the second peak in the A-scan. The time lapse between the two echoes returning to the transducer is deemed the time-of-flight (TOF). The TOF is measured by a specifically designed algorithm. By assuming the speed of sound to be constant in the material, the thickness of the simulated soft tissue could easily be calculated.

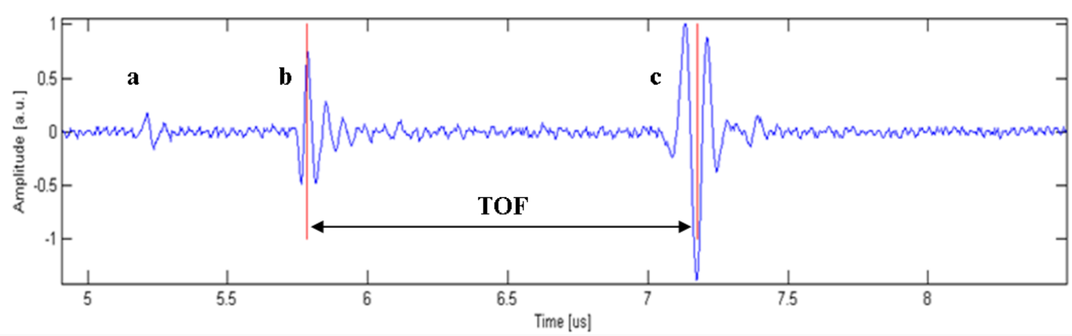

Figure 3.2 Example of an A-scan obtained from a phantom. Peak (a) shows an echo from the metal cap of the probe tip. Peak (b) represents the first echo from the surface, while peak (c) represents the second echo from the underlying bone.

According to the above example, all the system components must be specified and characterized to fit the requirements. Before being able to display the A-scan on the computer screen, the analog signal converted from the mechanical waves must be digitized.

The receiver block initially amplifies and adjusts the signal. The digitizer has a built-in analog-to-digital converter (ADC) and has additional circuits responsible for driving, buffering and transferring data to a computer. In the current systems, digital signal processors (DSP) and field-programmable gate array (FPGA) circuits are commonly used. A more detailed description about the acquisition process is provided later in the chapter.

3.2. An Ultrasonic Transducer – Characterization and Design Criteria

A typical ultrasonic transducer (a cross-sectional view) is shown [Fig 3.3].

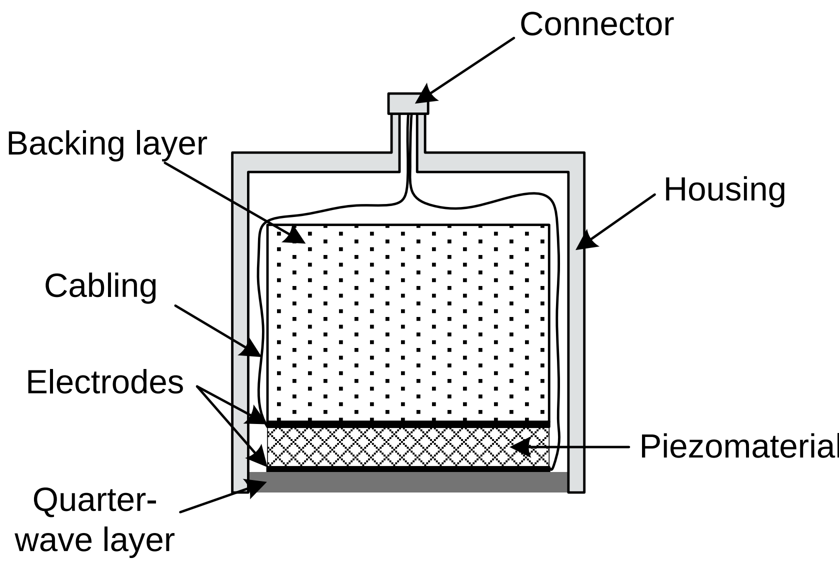

Figure 3.3 Cross-sectional view of a typical ultrasonic transducer.

A thin active piezoelectric material is covered from both sides with electrodes, which are connected to electrical wiring to transfer signals in and out of the transducer housing. The front face is usually protected by a so-called quarter wave plate. The back layer typically consists of an epoxy composite that acts as a highly attenuating material to prevent unwanted back reflections. Properties of the backing layer additionally control the shape and duration of the ultrasonic pulse. Several important technical parameters have to be specified during the transducer design:

- Piezoelectric material, central frequency, bandwidth and polarization orientation
- Housing dimensions, shape and connector type

- Focal distance (if focused) and the application environment

For further discussion just P-wave (pressure) immersion transducers are taken into consideration with the initially focused radiation surface.

3.2.1. **Piezoelectric Materials**

Over the decades, numerous research groups have been working on piezoelectric materials in order to improve their properties. In the early years, quartz was a common material carrying piezoelectric properties and it was initially used during World War I in sonar systems. Further developments have shown improvements in new materials such as barium titanate ($BATiO_3$) and lead zirconate titanate (PZT) which became the ultrasound materials used later due to their higher performance. A major milestone was achieved with the development of polyvinylidene fluoride (PVDF). The polymer foil, as opposed to ceramic or crystal, is easy to work with and it is relatively inexpensive. An important drawback is that the PVDF polymer has a lower coupling coefficient which means that it has a lower conversion rate from electrical to mechanical energy and vice versa, however, it has low acoustic impedance in order to match mechanically with the coupling medium (water).

Overall, based on the parameters [Tab. 3.1], it was decided that PVDF transducer is suitable for the system. The reason for this choice is mainly the mechanical and electrical matching to the system requirements, a broadband spectrum which effects in increasing the axial resolution, and overall performance of such material [56], [57].

Table 3.1 Generalized piezoelectric material parameters[1] [56], [57].

Material	k_t	$\varepsilon^s/\varepsilon_0$	ρ $\left[{kg}/{m^3}\right]$	c $[{m}/{s}]$	Q_m	Q_E	Z_a [MRayl]
PZT	0.60	201	3300	3943	9.2	25	13.0
PVDF	0.13	6.5	1.780	2150	12	4	3.87
$LiNbO_3$ crystal	0.49	28	4640	7340	10000	1000	34
$PbTiO_3$ ceramic	0.49	200	6900	5200	120	111	35.9

3.2.2. Spherically Focused Ultrasonic Transducer – Concept of Spatial Resolution[2]

As mentioned in the first chapter, the dimensions and object accessibility set the initial requirements for the transducer, followed by the requirements for the whole probe design. In order to discuss these criteria, the concept of resolution has to be introduced along with necessary definitions [Fig. 3.4].

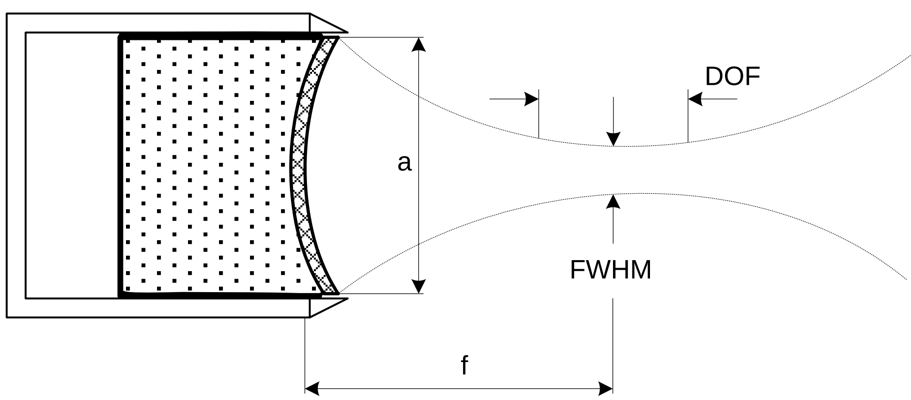

Figure 3.4 The beam properties of a spherically focused piezoelectric transducer cross-sectional diagram view.

The following are presented in figure 3.4:

- a – *aperture* – dimension of the active area of the piezoelectric

---

[1] k_t is the thickness mode electromechanical coupling coefficient; $\varepsilon^s/\varepsilon_0$ is the clamped dielectric constant; ρ is the density; c is the longitudinal wave velocity; Q_m and Q_E are the mechanical and electrical quality factors, respectively; and Z_a is the acoustic impedance.

[2] Transducer waveform and spectrum analysis is done according to test conditions and definitions of ASTM E1065

- f – *focal length* – distance from the lens to the focal point
- FWHM – *full width at half maximum* – diameter of the focal area, the level is set to -6 dB of amplitude in the focal plane
- DOF – *depth of field* – level set to -6 dB of the peak, on axis of the beam

The spatial resolution for spherically focused transducers is distinguished by an axial and lateral resolution, both are fundamentally different from each other but have equal importance.

In principle, the length (waveform duration) of the pulse produced by the transducer is what determines the axial resolution. It is usually assumed to be in the range of -20 dB of the peak signal amplitude (typically it is several wavelengths). It could also be expressed as a point spread function (PSF), which determines the minimum distance between neighboring details (layer interfaces) that can still be presented on the A-scan as separate objects (individual layers). For this reason, in a pulse-echo immersion setup, layer thickness x has to be larger than half of the pulse duration time multiplied by the velocity of sound.

The lateral (horizontal) resolution is characterized by the aperture and focal length. The F-number (also called, numerical aperture *N.A.*) of a focused transducer is defined as focal length (f) divided by transducer aperture (a). Finally, the FWHM is given by:

$$FWHM = \frac{1.41\lambda}{N.A.} \tag{3.1}$$

The axial and lateral resolution can both be improved by increasing the ultrasonic frequency. The drawback of that adjustment is that it limits penetration depth [50], [58]. The initial transducer trial tests were performed on a SAM setup with simple reflectors (glass slide with polyurethane layer on top).

3.3. The UDS Probe

The probe in the proposed system was designed for possible future use in a dental office. For this reason, additional requirements have been added to the system related to the shape and size of the transducer. For convenience, it was decided to use a continuous flow of water as a coupling medium for the prototype design. For the purpose of that design, a mini peristaltic pump was used with an electric motor and a controller. The appropriate software was designed along with the practitioners’ user interface to simplify the device operation.

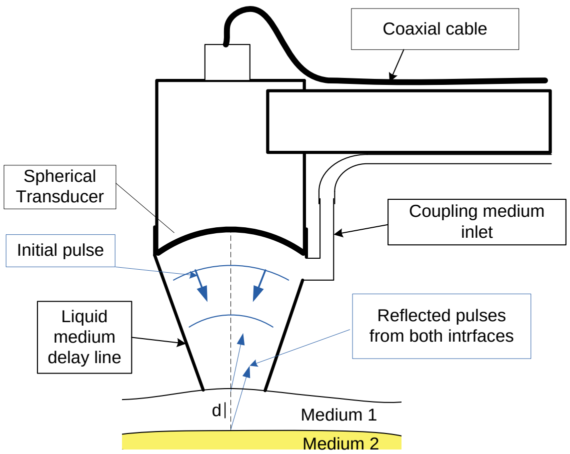

Figure 3.5 Schematic functional diagram of the UDS system probe.

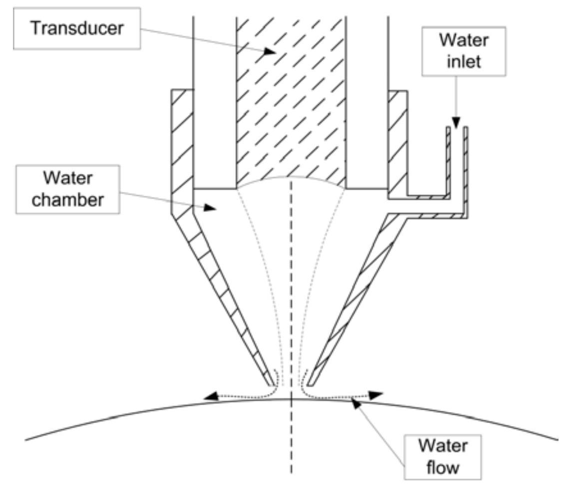

Figure 3.6 The transducer arrangement and the water flow in the delay line tip.

Figure 3.7 The fabricated UDS probe with the tip cup (delay line for coupling fluid).

In the proposed prototype, the probe head with the transducer mounted inside was angled to allow better angular adjustments in all directions during measurements. The delay line cup is disposable and can be changed to avoid possible cross-infections. The probe handle was designed and assembled taking into consideration the size and shape of existing dental tools.

3.4. A PC Ultrasonic Board: Pulser – Receiver and Digitizer

For the laboratory setup, specifically designed ultrasonic pulse generators are commercially available (for instance: Utex UT 340, Mississauga, ON, Canada; Panametrics 5073PR, Waltham, MA, USA). Usually, they are used to build the basic ultrasonic module when combined with an oscilloscope. More advanced PC ultrasonic boards, with built-in pulser-receivers and digitizers both microprocessor-controlled are utilized in commercial systems. Varieties of such systems exist but typically they are custom-made and designed for specific developments and applications. There are multiple requirements for these boards to be properly fitted for a particular application, and to work with specific transducer types.

An ultrasonic board consists of a digital and analog end and is responsible for generating and acquiring electrical signals. The pulser part on the board puts very short electrical impulses (~0.1 μs) having amplitudes on the order of several dozens of volts (needs to be optimized to particular transducer) [Fig. 3.8]. The repetition frequency of these pulses is mainly specified by the geometry of a measurement setup and usually does not exceed several kilohertz.

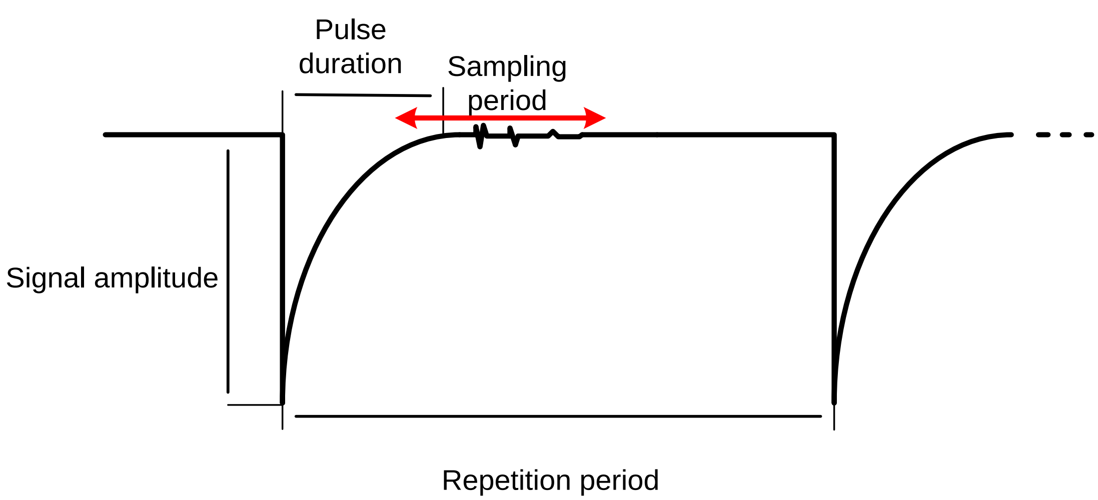

Figure 3.8 Characteristics of a typical electrical pulse generated in the ultrasonic pulse-echo system.

Pulses drive the ultrasonic transducer while, the electrical energy is converted into acoustical energy and then propagates as a beam of ultrasound. Scattered portions (echoes) of the initial beam are received by the same transducer in different moments of time and converted back to electrical signals. On the pulser end, an amplitude and duration of the initial pulse are the basic parameters, and usually fixed to standard values for simplifying the board power management.

Next, a transmitter/receiver switch separates the high voltage associated with pulsing from sensitive initial amplifiers on the receiving side. In current systems, it is usually integrated in one package with a pulsing circuit (for example microchip Supertex HV7361). Afterwards, the signal is initially amplified, and filtered if necessary, to fit the input range of an ADC converter. The amplification is usually performed in a couple of steps by both constant and variable gain amplifiers. The commercial impact on ultrasound instruments is so prominent that major circuit manufacturers develop integrated chips with multiple gain stage amplifiers built specifically for ultrasound applications (an example is the mentioned Supertex chip).

Finally, the last step is for the signal to be digitized. The ultrasonic system itself sets the criteria for the ADC converter, primarily the sampling frequency and the vertical resolution. In principal, to avoid aliasing, the Nyquist theorem requires analog signals to be sampled with a frequency two or more times higher than resonant transducers' frequency. In practice, for ultrasonic systems, a sampling rate 4-5x higher than the resonant frequency is acceptable [59]. The second parameter is the sampling resolution, which establishes the minimum voltage step size within a voltage range. Common values are 12-, 14- and 16- bits and usually it is traded with the amount of samples to be possibly acquired in a second. If the ADC converter has 2 V_{pp} input range and 12-bits resolution, then the minimal step is equal to 0.49 mV.

In the older but still cost effective systems, an oversampling (also called, super-sampling) protocol was proposed. Ultrasonic signals have the important feature of being repetitive, so that just a portion of information could be captured during one acquisition. A small time shift between each repetition of the signal can be applied to achieve super-sampling. The drawback in this case is the time necessary to acquire a single A-scan. If this were not the issue, this method could lower requirements for ultrasonic systems along with their cost.

3.5. Software Development

The software development can be distinguished by its signal detection algorithm, hardware control, and user interface. The current stage of the prototype has an integrated coupling medium delivery block and ultrasonic board control. Both have available programming libraries and manuals for developers.

The interface was designed with the help of the feedback received from dental practitioners and implemented in the Microsoft Blend® interface creator. The functional code was programmed in C# with using .NET libraries in Microsoft Visual Studio® programming environment [Fig 3.9].

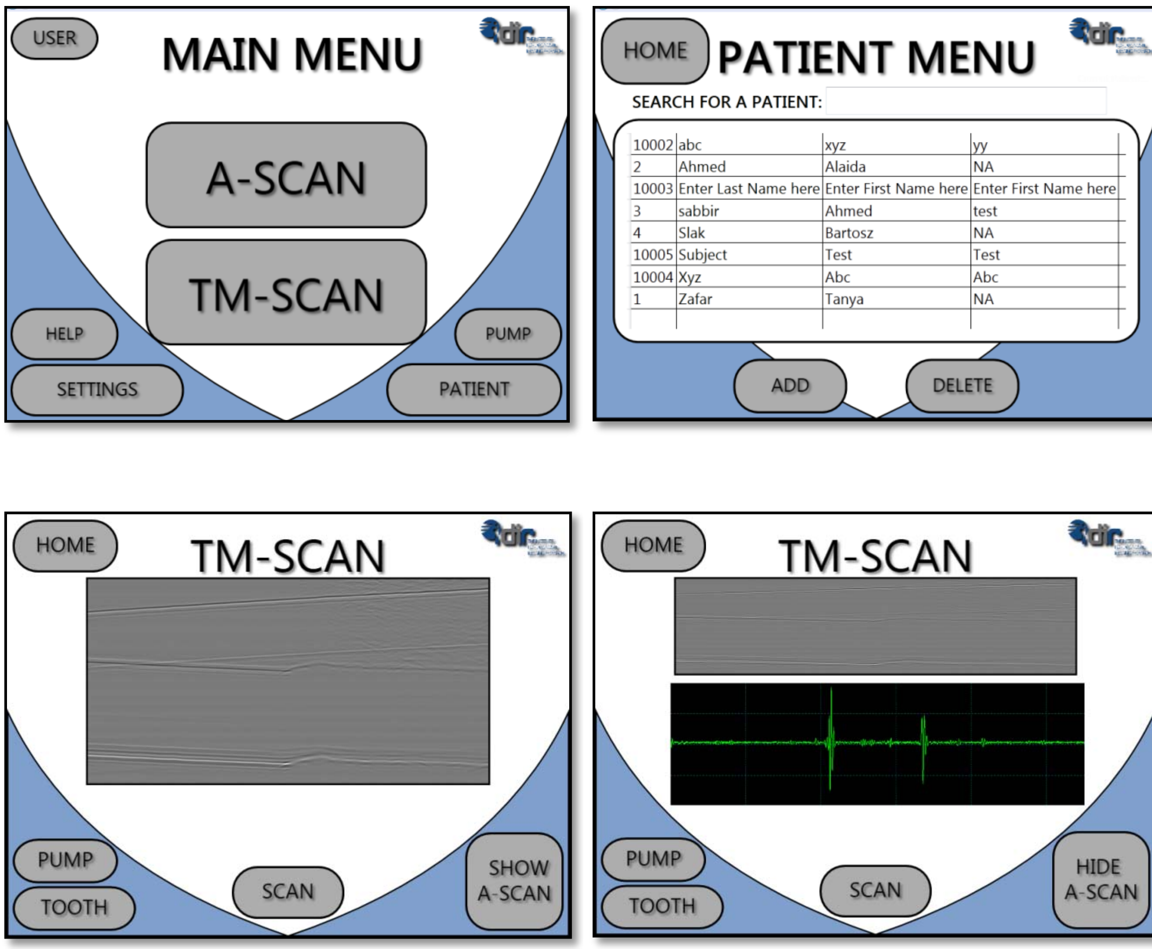

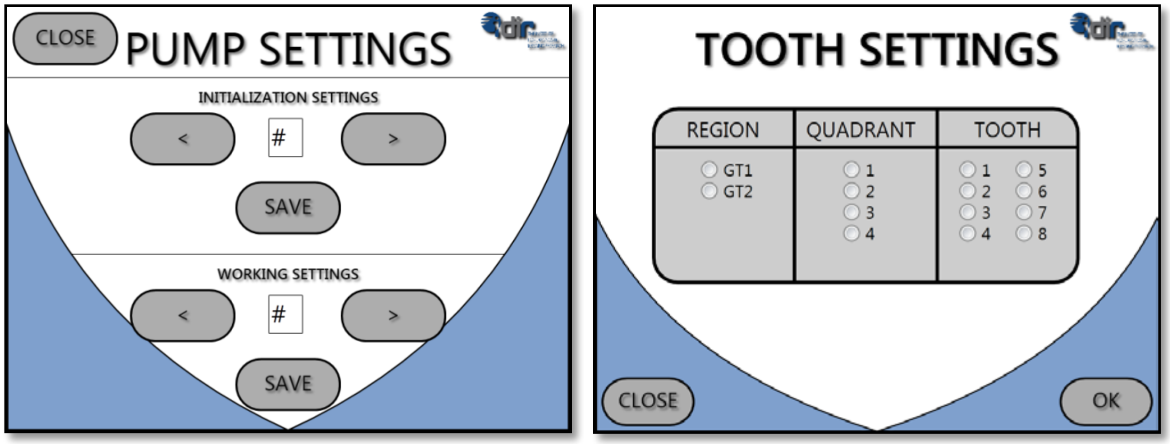

Figure 3.9 Preliminary UDS interface screenshots.

3.6. The Ultrasonic Dental System – Testing

At first, a prototype of a compact ultrasonic system was designed and built. This system consisted of an analog and digital circuit with a display screen and embedded computer. The hand-held probe was equipped with a 50 MHz ultrasonic transducer built into a pen-like housing. Spherically shaped PVDF piezoelectric film was used as the transducer material. The acoustic focal point formed allowed one to achieve optimal lateral resolution and accurate localization over the targeted tissue. Water was able to flow continuously through the probe from a built-in pump, eliminating the requirement for ultrasonic coupling gel. The entire system can be placed on a small tabletop in the practitioner's office and requires only an external power source [Fig 3.10].

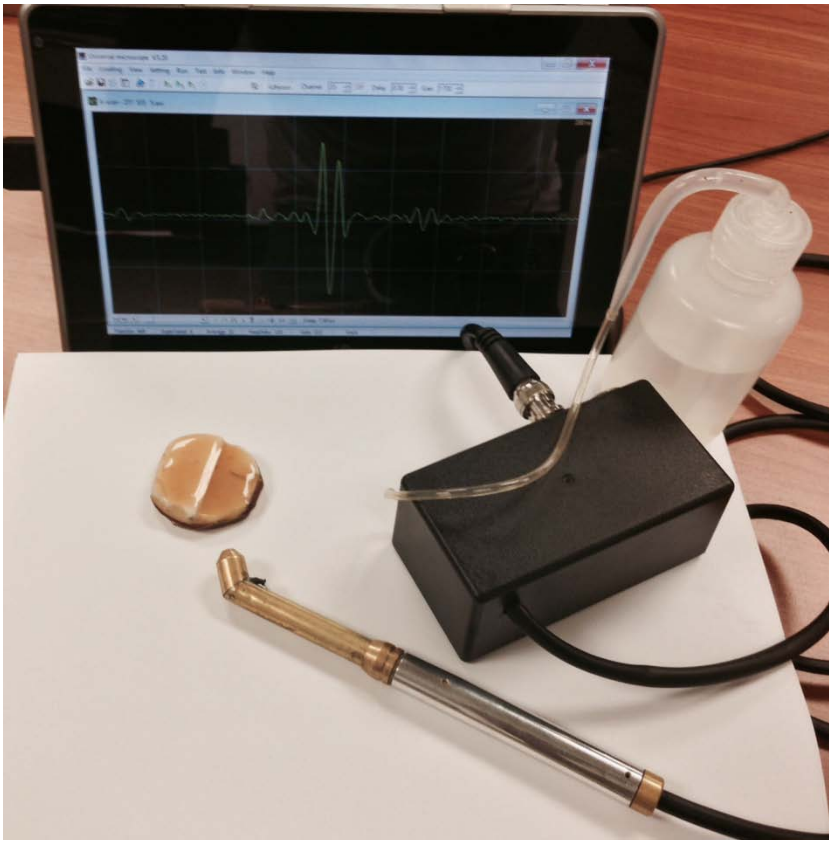

Figure 3.10 The UDS prototype with the probe and the water pump module.

3.6.1. Soft and Hard Tissue Phantom Testing

A phantom simulating oral soft tissue over an alveolar bone was constructed. The oral soft tissue was simulated by polyurethane layer since this material has similar ultrasonic properties [60]. The bone was made irregular and non-uniform, to simulate the texture of the alveolar process [61]. Ten locations were marked in a line along the polyurethane surface and each location was presumed to have a different thickness. Ultrasonic measurements were first obtained by localizing the probe tip over each location. Next, invasive measurements were taken at each location (described in details in later chapters). For these ultrasonic and invasive measurements, each location was measured ten times to build a statistical database. In addition to ultrasonic and invasive measurements, a cross-section along the line of points was made and direct measurements of thickness were obtained from images taken with an optical microscope

(Keyence VHX 2000E, Itasca, IL, USA). Deviation associated with the direct method was calculated based on multiple measurements obtained using computer software.

Measurements obtained from the ultrasonic method were close in value to those obtained from the invasive and optical microscope. In the majority of cases, however, ultrasonic measurements of thickness were slightly larger than invasive measurements. In the majority of trials, error was greater for the invasive method [Tab. 3.2, Fig. 3.11].

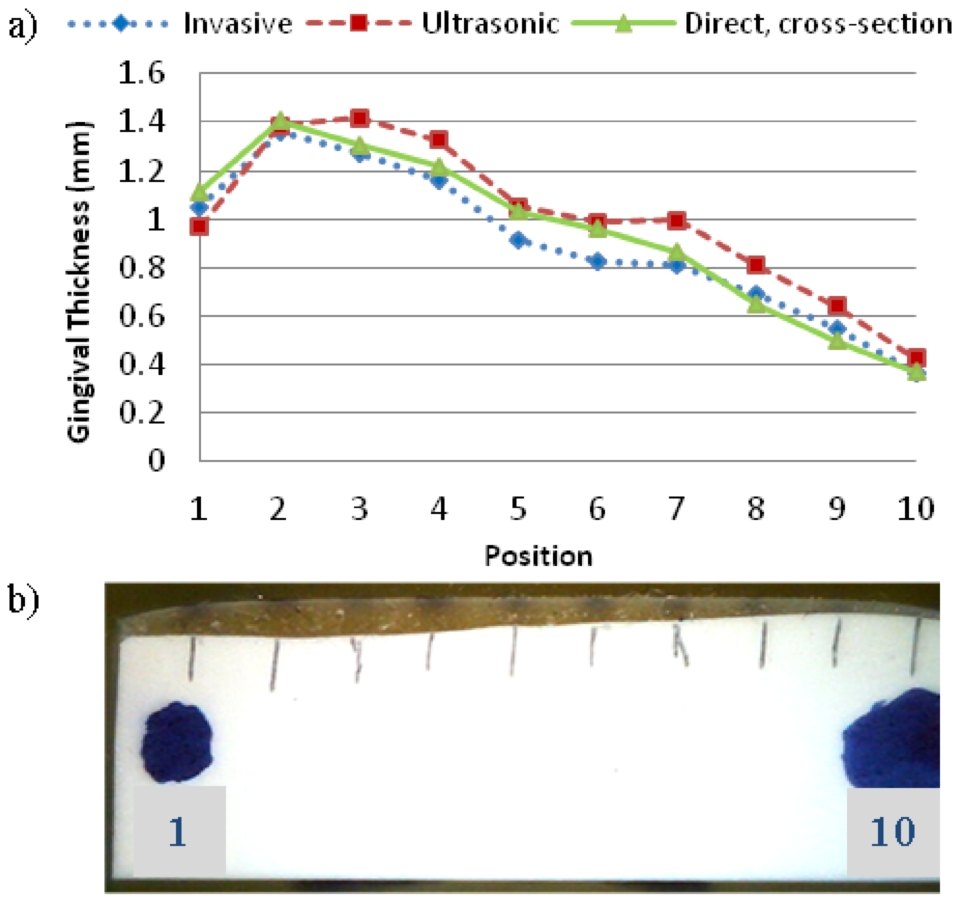

Figure 3.11 a) Average GT values for positions along the phantom, obtained from three methods (for legibility, error is presented in table 3.2) b) The microscopic cross-sectional image used for direct thickness assessment.

Table 3.12 GT values (in mm) for phantom tissues are shown as averages for each position, along with standard error. Error associated with the direct method is not presented since error values were on the order of microns.

Position	1	2	3	4	5	6	7	8	9	10
Invasive	1.05 ± 0.04	1.36 ± 0.06	1.27 ± 0.02	1.16 ± 0.02	0.92 ± 0.01	0.83 ± 0.04	0.81 ± 0.03	0.69 ± 0.04	0.55 ± 0.02	0.36 ± 0.02
Ultrasonic	0.97 ± 0.01	1.38 ± 0.01	1.42 ± 0.01	1.32 ± 0.02	1.05 ± 0.01	0.99 ± 0.01	0.99 ± 0.01	0.81 ± 0.01	0.64 ± 0.01	0.43 ± 0.02
Direct, cross-section	1.11	1.41	1.31	1.22	1.03	0.96	0.86	0.65	0.50	0.37

3.7. Summary

High-frequency ultrasound technology has the potential for detailed delineation of anatomical structures. Areas of interest pertaining to this case include organs (body parts) of small size, like eyes, skin, vascular structures or the proposed periodontium tissue and teeth. The requirement, and at the same time limitation of an ultrasonic system for all of these applications is the trade-off between depth of wave propagation and system resolution.

For this reason, for UDS, a focused transducer was built with the following parameters:

- 50 MHz central frequency
- 100 % bandwidth
- 7 mm focal point distance
- 12° half angular aperture

The transducer was designed and custom-made for the purpose of this study. For simplicity of fabrication based on available materials and facility equipment the probe was made out of polished aluminum and brass tubes. However, for the future prototype developments, a polymer will be taken into consideration. The UDS was designed and assembled as well as initially tested on phantoms mimicking soft and hard dental tissues.

CHAPTER 4.

THE EXPERIMENTAL STUDY – HARD AND SOFT DENTAL TISSUE DIAGNOSTICS

This chapter presents the experimental study performed on soft and hard dental tissues using the UDS developed. An enamel and gingival thickness were also ultrasonically assessed.

In general, knowledge about exact thickness of these tissues allows practitioners to adopt the most suitable procedure and to better predict the quality of a final restoration. Both these applications are motivated by examples of real dental procedure requirements described in this chapter.

Laboratory experiments were performed on porcine cadavers slaughtered for consumption purposes. The setup arrangement was to resemble a dental office environment and portray its limitations. All results were validated through invasive and destructive measurements (where applicable).

4.1. Hard Tissue Experiment – Enamel Thickness (ET) Measurements

4.1.1. Motivation and Background

Dental veneers are thin layers of plastic, composite or ceramic material bonded over a specifically prepared tooth surface [62]. According to the common placing procedure, most veneers require partial removal of the enamel layer from the front surface of the tooth before restoration [Fig. 4.1]. For a healthy tooth, it is recommended to remove at least 0.6 mm of the enamel [63]. It is also suggested that the thickness of the adhesive cement, which is used to fix the veneer onto the ground surface of the tooth, should not exceed 50 µm [64] (i.e. it does not affect the thickness of the enamel layer required to be removed before restoration).

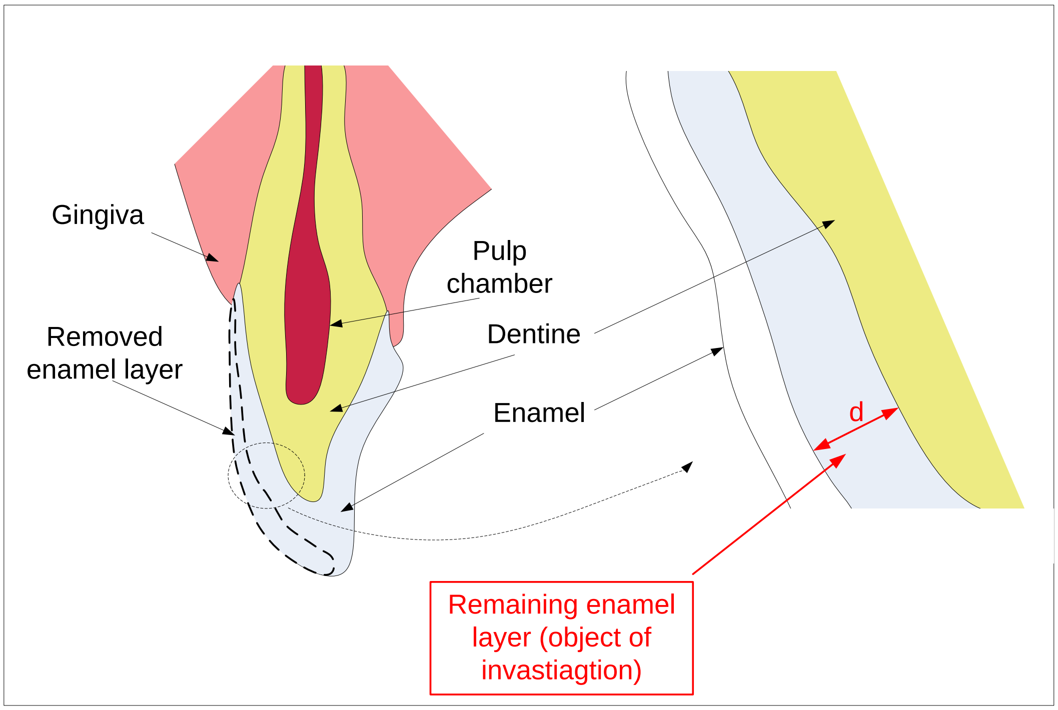

Figure 4.1 The schematic diagram of an axial cross-section of an incisor: dashed line shows the enamel layer to be removed during the veneer placing procedure. Right: close-up view of the enamel to be measured.

It is well established that bonding to the enamel layer is much better than to dentin regardless of the dental adhesive system, thickness of the cement layer or veneer laminates [65], [66]. Therefore, it is extremely important to know the thickness of the enamel layer remaining after grinding to ensure the quality of restoration [Fig. 4.2, Tab 4.1].

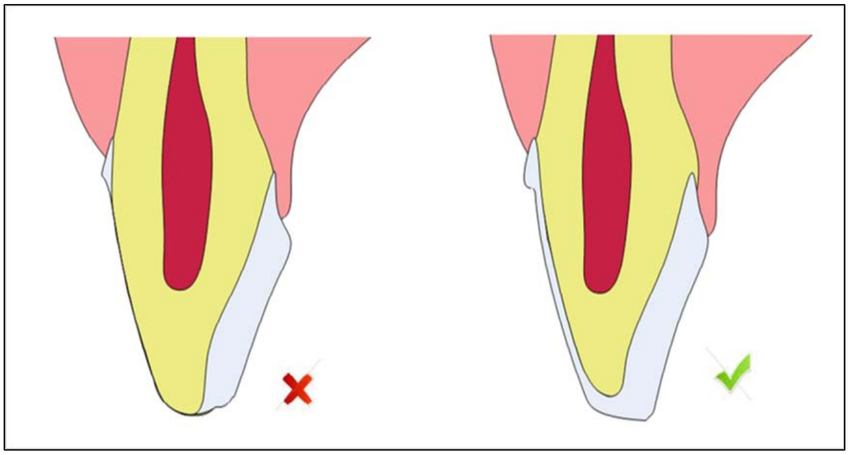

Figure 4.2 Cross-sectional view of the enamel surface preparation for veneer placement procedure.

Table 4.1 Comparison between enamel surface conditions for a veneer placement procedure.

When dentin is exposed:	**When a thin enamel layer remains:**
· elevated postoperative tooth sensitivity	· superb strength and smoothness
· high odds of veneer debonding	· no discoloration
· possible pulpal damage	· excellent retention of veneers
· unpredictable changes in occlusion	· long-term success

At this time, dentists do not have any non-invasive tools enabling enamel layer measurements in a chosen spot [35]. Dentists can rate oral health using special indexes [67], [68] and statistically estimate the enamel thickness, but without any numerical values and certainty of the estimation. The UDS system can help perform fast and reliable measurements without using harmful radiation as well as complex and expensive equipment. In recent publications related to ultrasonic enamel thickness measurements, the central frequency of the transducers used in evaluations were in the range of 10 to 35 MHz [24], [35], [69], [70] which resulted in limited axial and lateral resolution.

The objective of this experiment was to investigate the ability of a high-frequency ultrasonic transducer-based, hand-held probe in UDS for thickness measurement of the enamel remaining after grinding of the tooth surface.

4.1.2. **Materials and Methods**

In the experiments conducted, porcine teeth samples were used. To avoid the influence of the environment on the experimental results, all specimens were kept in the same liquid (5 % thymol solution). The UDS system was used for the measurements of these samples. Additionally, an optical microscope was used for direct measurements of the enamel layer thickness in the exposed cross-sectional areas.

The measurement procedure can be explained as follows. The thickness of the enamel layer d can be calculated from the simple relationship: $d = \Delta tc/2$ (where Δt is round-trip time and c is the speed of sound in enamel). The first parameter, the round-trip time, was determined by measuring the time delay Δt between the echoes from the surface of the sample and the DEJ interface. The second necessary parameter is the sound velocity c, which depends mainly on the mechanical properties of the medium. It was proven in literature that the dental enamel is anisotropic [4], [71], [72], [73], and its features depend on several factors (e.g. alignment of fiber-like apatite crystals, demineralization, the sample storage liquid, etc.). For this reason, multiple literature sources report different values of the velocity of sound in the dental enamel, which is usually assumed to be in the range of 5900 ±300 m/s. The differences in the observed sound velocity values can also be due to the fact that certain alignment corrections are necessary before the probe is positioned perpendicularly to the surface to get an appropriate waveform with recognizable signal from the EDJ [23].

In the current investigation, the velocity of sound was measured using the following approach. At first, one of the tooth samples was cut down the long axis of the tooth to expose the cross-sectional area, allowing direct measurement of the enamel thickness with the optical microscope [Fig. 4.3].

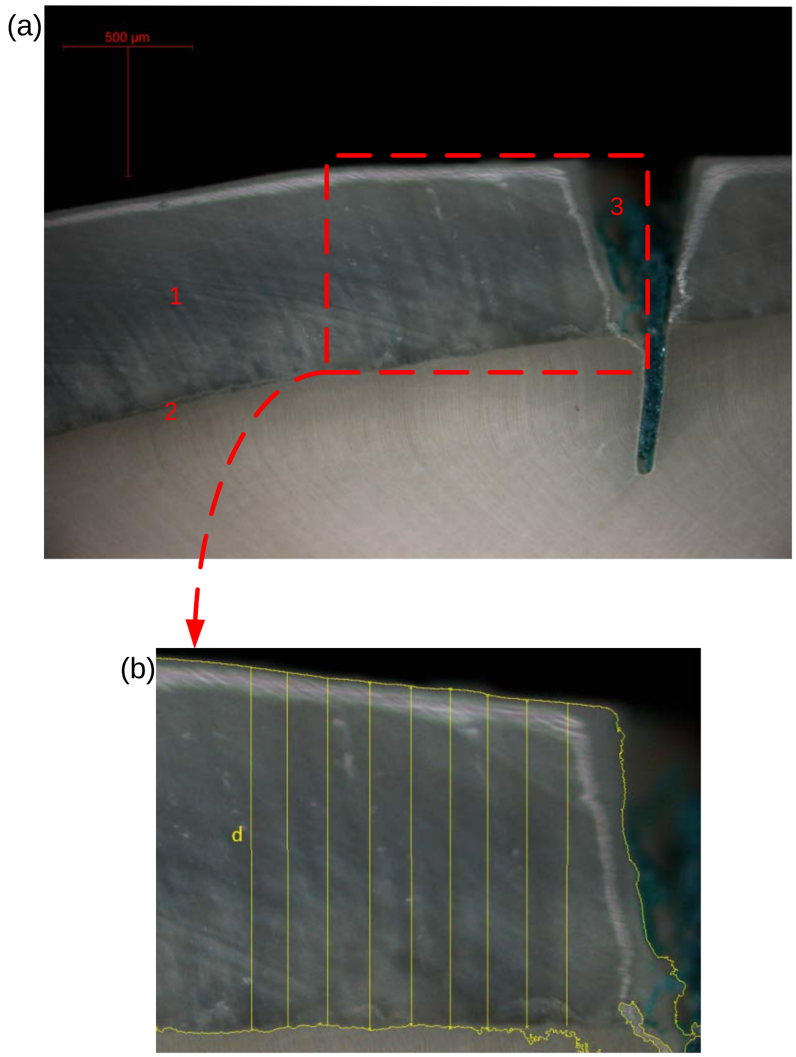

Figure 4.3 (a) Optical cross-sectional image presenting enamel layer (1), enamel-dentin interface (2), and marker cut (3); (b) close-up view of the measurement area (d - the enamel thickness).

Then the same cross-sectional area of the tooth sample was analyzed using the SAM [Fig. 4.4] and the round-trip time was determined. It is important to note that the suitable waveforms were selected by carefully adjusting the position of the sample and the results were recorded only if the operator deemed the wave to be satisfactory. Knowing the distance (i.e. the enamel layer thickness) and the round-trip time, it was possible to estimate the velocity of sound in particular samples to be 6200 ±120 m/s and this value was used in further calculations. The properties of the enamel were assumed to be homogenous and isotropic. Therefore, a constant value of the velocity of sound was used in calculations. This approach allowed, considering the time of flight and proper localization of the ultrasonic beam path, the main uncertainties influencing the accuracy of further measurements.

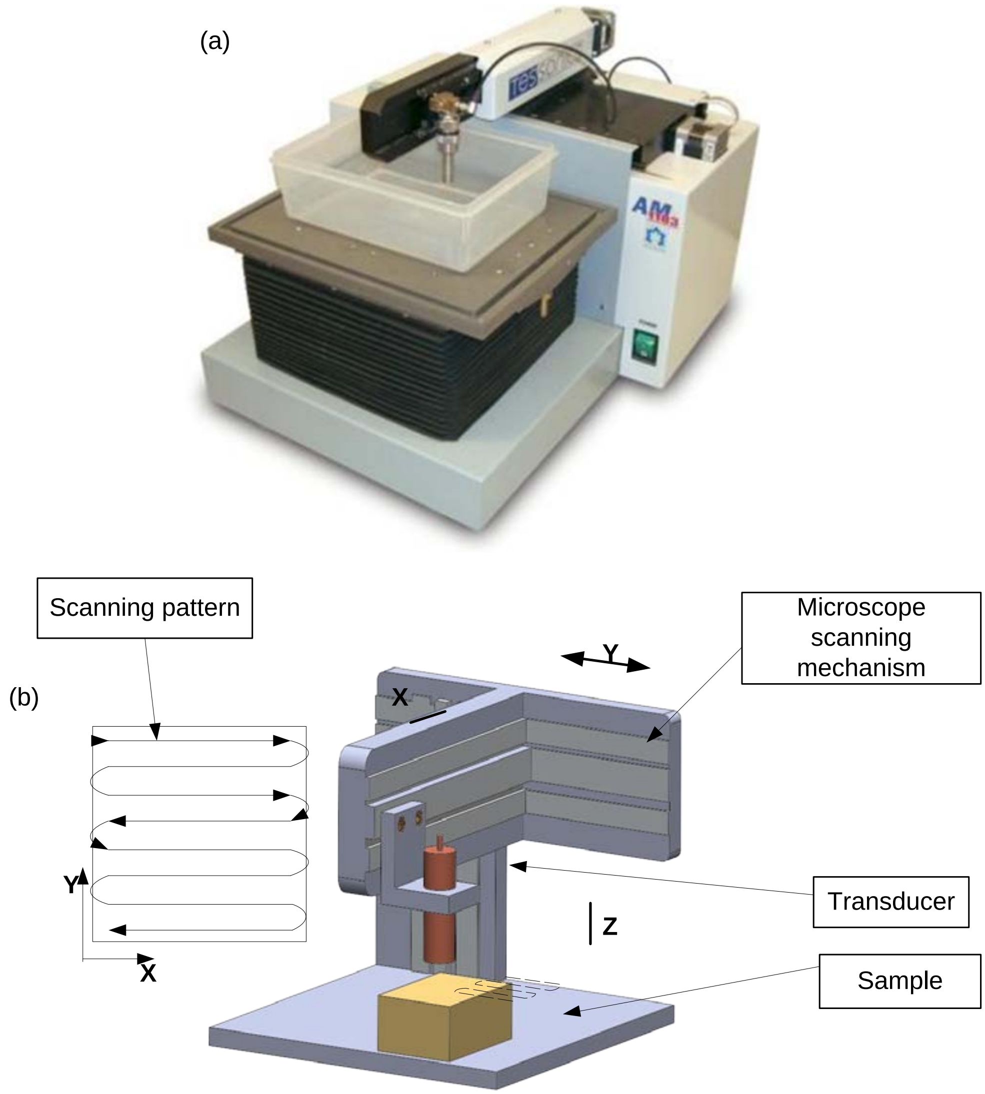

Figure 4.4 (a) An acoustic microscope used in experimental work (Tessonics AM1103, Windsor, ON, Canada) (b) Illustration of the scanning technique.

Due to the fact that enamel layer is not uniform over the tooth surface, special markers were made to localize the position of the ultrasonic beam on the surface of the tooth samples. Two notches (along and across the tooth) were cut on the surface of each tooth by means of a special linear saw (Wire Saw WS-22, K.D. Unipress, Poland). The notches were 0.15 mm wide, enough to be clearly noticeable on the surface of each sample. A practicing dentist was asked to prepare samples to study the ability of the hand-held probe to measure the thickness of the remaining enamel layer after grinding (the intention was to remove the thin enamel layer, in accordance with the veneer placing procedure [74]). The same grinding tools as in the dental veneer placing procedure were used for that purpose. The measurements were taken before and after grinding the samples. The observer attempted to position the probe tip for each of the measurements in the 2x2 mm area determined by the mentioned notches [Fig.4.5].

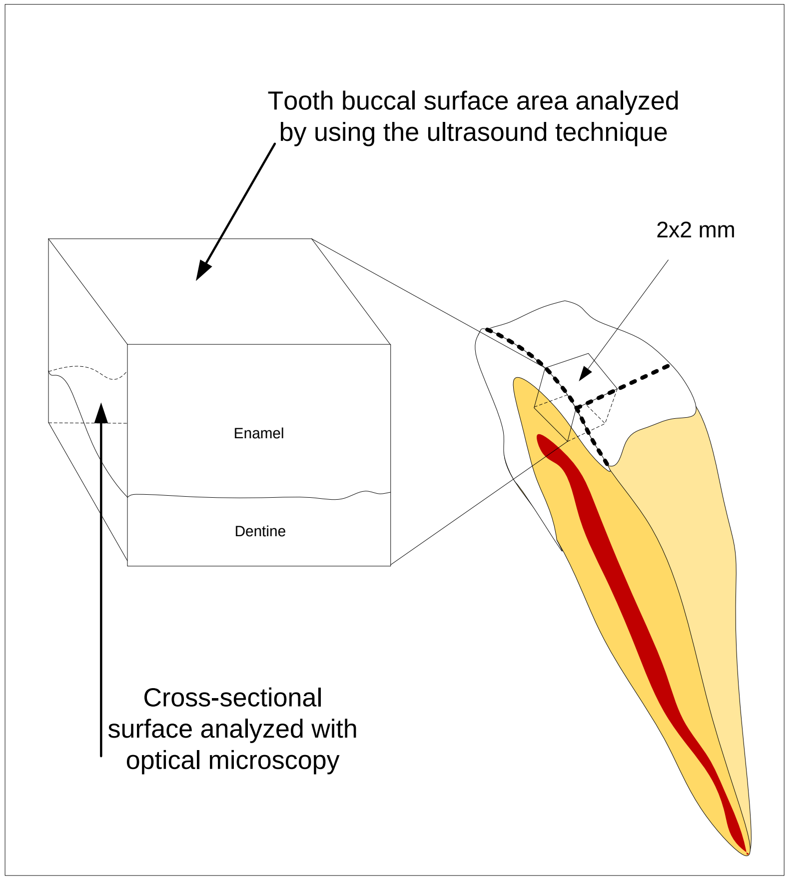

Figure 4.5 A schematic diagram of the experimental surfaces.

The second part of the experimental work was to verify the “sensitivity” of the ultrasonic measurements to the consequent grinding of the enamel. At first, a separate sample was cut down the vertical notch and the thickness of the initial enamel layer was measured by the optical microscope from a cross-sectional view. Next, the enamel thickness was determined in the 2x2 mm area by using the UDS. After each consecutive grinding of the tooth sample, the measurement process was repeated.

4.1.3. **Results for ET Measurements**

Average values of enamel thickness measurement are shown [Fig. 4.6].

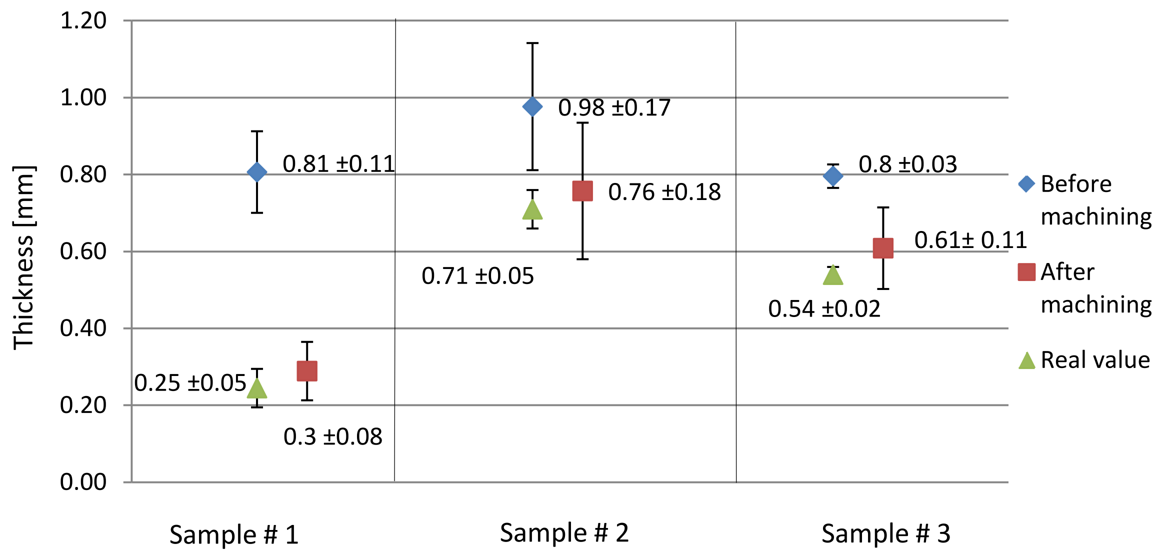

Figure 4.6 Average values of the enamel layer thickness measurements obtained with the UDS, before and after the machining process compared to cross-sectional thickness measurements.

For sample #1, the results show that it was prepared correctly since the dentist removed approximately 0.5 mm of the material and the thickness of the remaining enamel layer was enough to "insulate" the veneer from the dentin. For the other two samples less enamel material was removed than was intended. To verify the results of ultrasonic measurements, after grinding, each of the three samples was cut down the long axis, so that the enamel layer could be measured by the optical microscope ("Real values" shown [Fig 4.6]). The results obtained with the optical microscope have significantly lower uncertainties since the enamel thickness was measured directly along the edge of the cross-section, exposing the EDJ.

The enamel thickness values before and after grinding are shown [Fig 4.7].

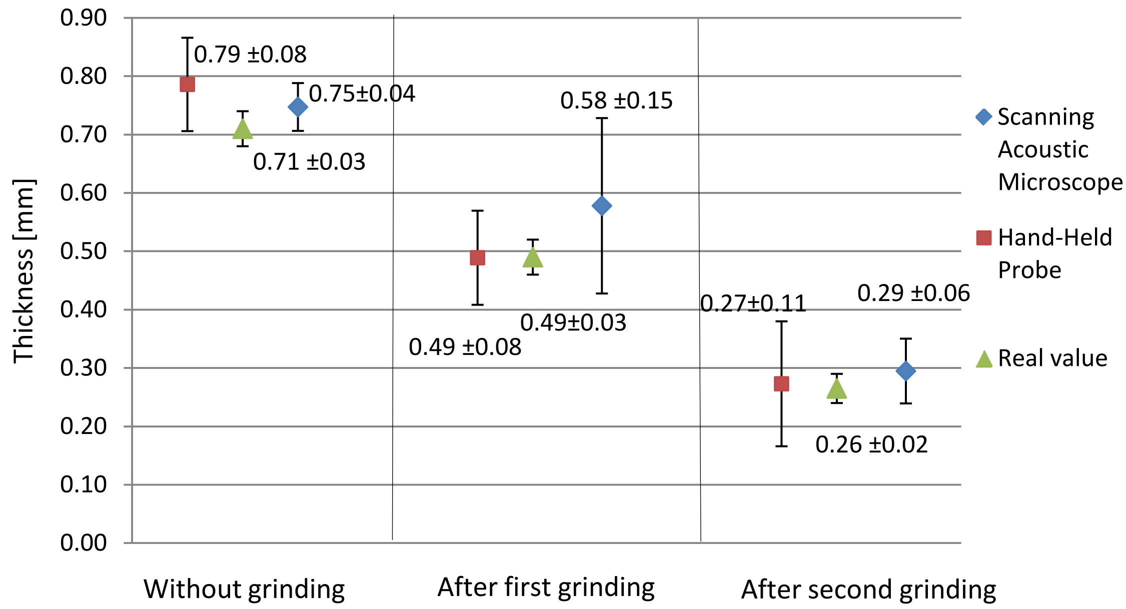

Figure 4.7 The enamel thickness values: initial and after first and second grindings of the tooth surface.

It can be verified that the enamel thickness values received from the hand-held probe and the acoustic microscope are close. The average discrepancy was 5, 16 and 5 %, respectively. The difference between the enamel thicknesses obtained with the optical microscope ("Real value") and the values measured by the hand-held probe were 10 % or less. Taking into account uncertainties, the results in both cases are practically independent of the level of grinding, hence supporting the possibility of applying the ultrasound technique in this specific enamel thickness measurement application.

4.2. Soft Tissue Experiment – Gingival Thickness (GT) Measurements

4.2.1. **Motivation and Background**

The importance of taking into account the differences in GT during surgical and non-surgical treatment planning has been widely recognized since thick and thin periodontal biotypes respond differently to inflammation, restorative trauma, and surgical insult [75]. However, methods currently used to discriminate thick from thin gingiva have limited reliability and accuracy [76]. During periodontal diagnosis, keratinized gingiva and unattached mucosa covering the periodontium are assesed. This knowledge allows the practitioner to adopt the most suitable procedure. One such instance is the gingival recession coverage, whereby the tissue grafting must be performed [77], [78], [79]. In cases where GT is less than 0.7 mm in recipient sites, the translation method should be avoided. Preferably, a method using autogenous connective tissue grafting should be implemented [80]. On the other hand, GT greater than 1.1 mm has a greater chance for successful coverage, namely using the coronal positioned flap method [81]. In orthodontics, GT assessment prior to the application of orthodontic forces is important as such knowledge can prevent complications arising from gingival recession [82] [Fig. 4.8]. Other instances include performing control guided bone and periodontal tissue regeneration using membranes and preparing surfaces for denture installation [83].

Figure 4.8 An example of multiple advanced pathological changes in gingiva and bone (gingival and bone recession) occurred four years after orthodontic treatment due to incorrect teeth repositioning protocol (treatment was performed without properly diagnosed gingival thickness and position of the bone crest) (*Courtesy of Dr. Bednarz*).

Several methods are available for GT assessment. For the initial diagnoses, a ratio between the length and width of middle incisors is determined, as well as between keratinized gingiva and papilla width [84], [85]. Another technique which is similar to a visual assessment is the transparency method [84]. Although these methods provide valuable information, they do not involve direct measurements. More reliable GT assessment is provided by invasive and non-invasive techniques. A common invasive method involves transgingival probing of locally anesthetized tissue with a k-file endodontic needle [47], [83], [86], [87]. Another invasive method is X-ray CT which does not require anesthesia [87].

Table 4.2 Thick vs. thin gingival tissue in surgery, tooth extraction and inflammation.

	THICK	THIN
Inflammation	Soft tissue: - cyanosis (lack of oxygen) - bleeding upon probing Hard tissue: - bone loss with pocket formation	Soft tissue: - marginal redness - gingival recession Hard tissue: - rapid bone loss
Surgery	Healing predictable	Difficult to predict whether tissue will heal
Tooth extraction	Minimal ridge degradation	Ridge degradation

4.2.2. **Materials and Methods**

A porcine jaw was used in the experimental work. The jaw was refrigerated immediately upon the animal's death and experiments were performed within a twenty-four hour period. An array of measurement locations was marked on the buccal gingival surface in the fourth quadrant: GT1 locations were those in the middle of keratinized gingiva and GT2 locations were those in the alveolar mucosa approximately 2 mm apical to the mucogingival junction [86]. Ultrasonic trials were performed ten times at each location and invasive trials were performed once at each location to mimic standard dental protocol [83]. The reading error between invasive data was the result of measuring the displacement of the rubber limiter with computer software ten times per measurement.

For invasive measurements, #25 k-file endodontic needles were used (Diadent Group Int., Burnaby, BC, Canada). The needle was inserted perpendicularly into the gingival surface at the marked location. The limiter remained at the gingival surface while the needle proceeded through the soft tissue until bone or cementum was hit. The needle was then removed and the distance between the rubber limiter and the tip of the needle was measured. This was done by taking an up-close photograph of the displaced limiter adjacent to the thickness reference block (Albuquerque Industrial, Forest Hills, NY, USA) and using computer software to measure the limiter displacement. This distance was taken to be the thickness of the gingiva [88].

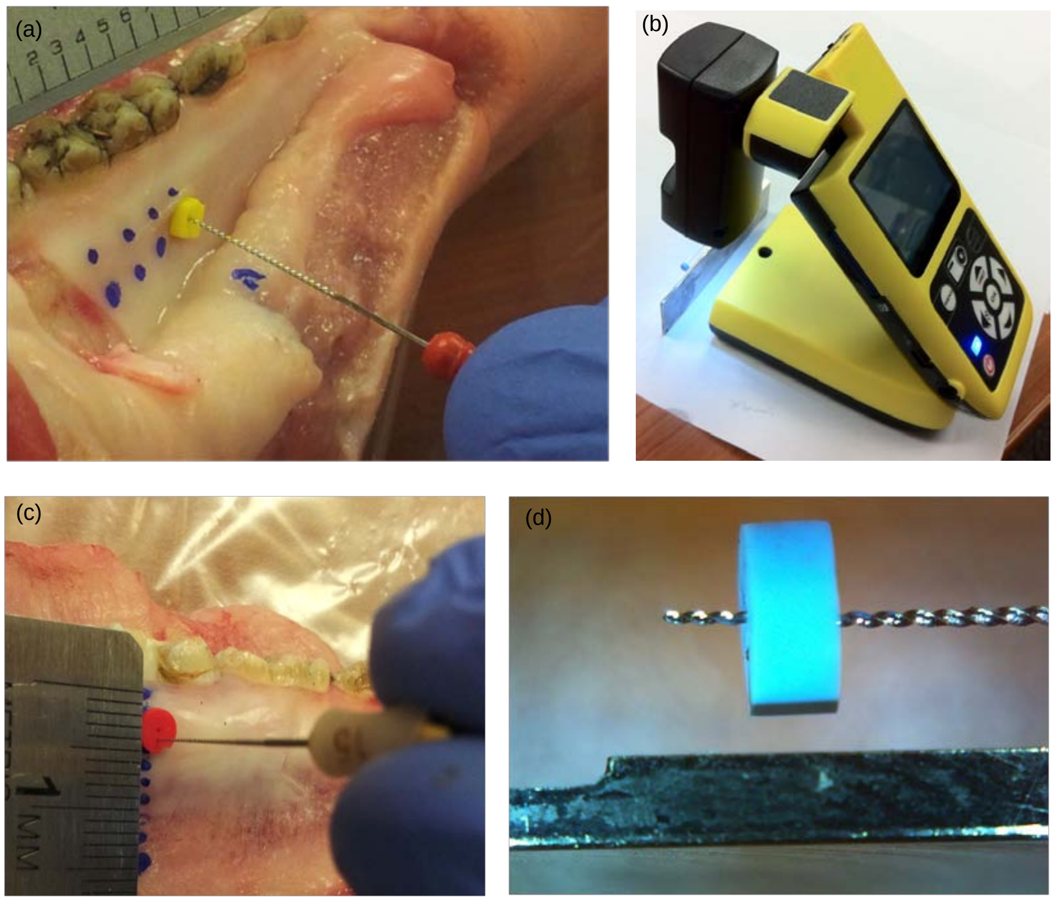

Figure 4.9 (a) Mandible with k-file; (b) Micro-camera; (c) Measurement points marked along gingiva with k-file; (d) The close-up view of the k-file needle with the reference measurement block.

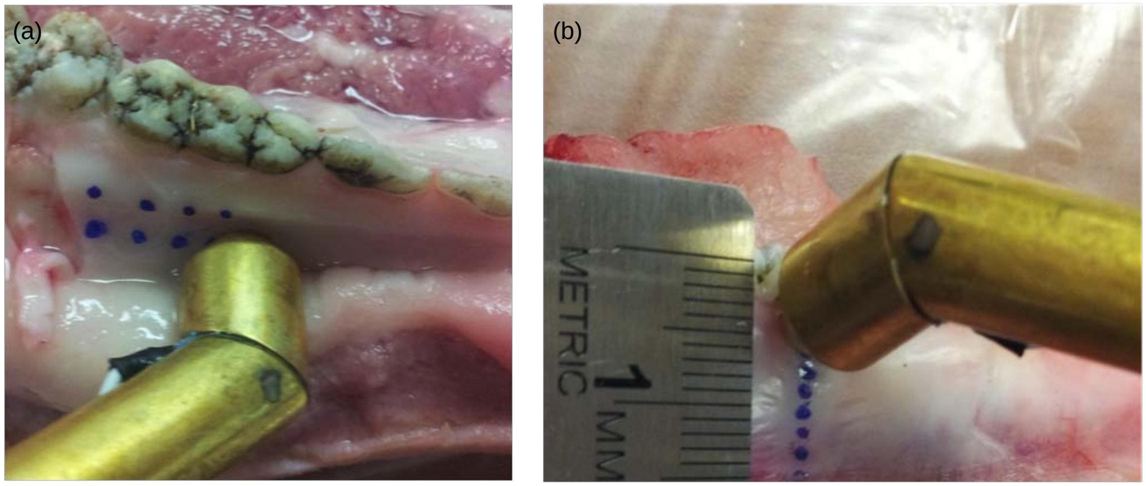

Figure 4.10 The UDS system probe localized in the marked measurement spots: (a) Experimental trials for GT1 and GT2 positions; (b) Vertical line ultrasonic measurements for bone crest detection.

Lastly, a vertical line measurement experiment was designed and performed to prove applicability of the system for the position detection of an alveolar crest in close proximity with teeth, and eventually implants. Especially from the labial side, it has a significant importance before, during and in the maintenance phase of treatment for determining bone loss and regeneration processes [89], [90], [91]. For instance, in implantology the lack of bone or a significant loss is one of the success rate criteria of the treatment [92]. The bone crest level and its thickness are factors that determine the possible formations of gingival recession in the future [89]. Dehiscence is defined as a bone loss of at least 4 mm in height in respect to interproximal crestal bone [Fig 4.11] [93].

Figure 4.11 (a) An example of bone pathological changes - dehiscence and fenestration (bone windowing); (b) Measurement points marked along gingiva for bone pathology detection on porcine cadaver sample.

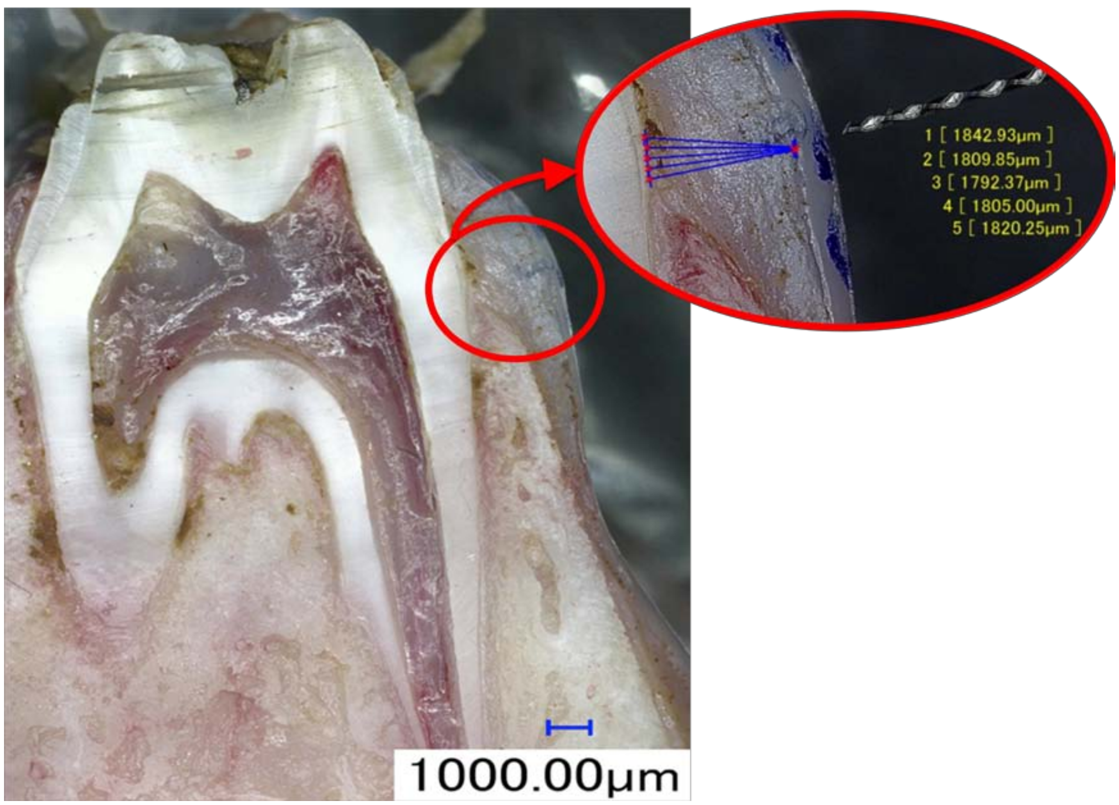

Figure 4.12 The cross-sectional view of a sample periodontium followed by a close-up view of the thickness measurement procedure and error estimation.

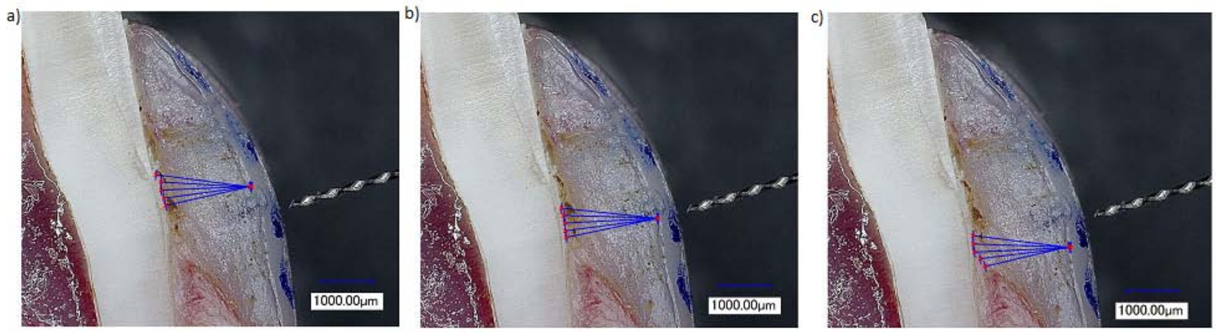

Figure 4.13 Direct assessment of GT was performed by obtaining a high-resolution, cross-sectional image of the periodontium along the line of points. For each of the twelve measurement locations, GT was directly measured at three groups per POI: (a) the group of five measurements coronal to the centre of the dot, (b) the group of five measurements at the centre of the dot, and (c) the group of five measurements apical to the centre of the dot. The # 20 k-file needle is also shown.

Prior to all the experiments, the speed of sound in a gingival sample was estimated. The SAM operating in B-scan mode was used to obtain TOF values. A sample of gingiva was excised from the buccal surface in the fourth quadrant. The sample was placed between two parallel, glass microscope slides while immersed in water at 20 °C. Twenty measurements of TOF were taken at equal intervals through both water and tissue. The speed of sound in water was assumed to be 1482.34 m/s at 20 °C [94]. By having obtained the TOF through water, the distance between the microscope glass slides could be calculated, which was assumed equivalent to the thickness of the gingiva sample. Finally, using this obtained value for thickness along with the measured TOF through tissue, the speed of sound through porcine gingival tissue was determined [Fig. 4.14]. The speed of sound in a single porcine gingival tissue sample was calculated to be 1564 ± 21 m/s.

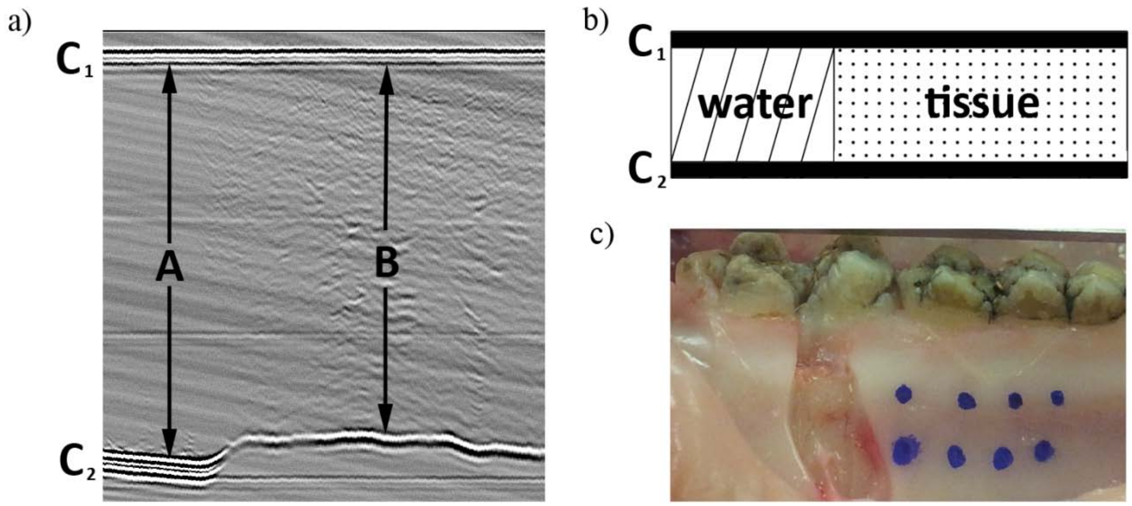

Figure 4.14 (a) The B-scan showing (A) TOF through water and (B) TOF through gingival tissue, held in place between microscope slides (C1 and C2). Note the speckle appearing in the image of the tissue resulting from a non-uniform histology through the sample. Average TOF values through water and tissue were 1.32 µs and 1.25 µs, respectively (b) A schematic representation of the experimental setup (c) The site on the buccal gingival surface of the fourth quadrant from which tissue was excised.

4.2.3. **Results for GT Measurements**

Results show a decent overlap of values. GT1 locations were found to be thicker than GT2 locations as determined by both methods. Maximum error in thickness for all ultrasonic data was 10.3 % for the GT2 location in position II [Tab. 4.4, Fig. 4.15].

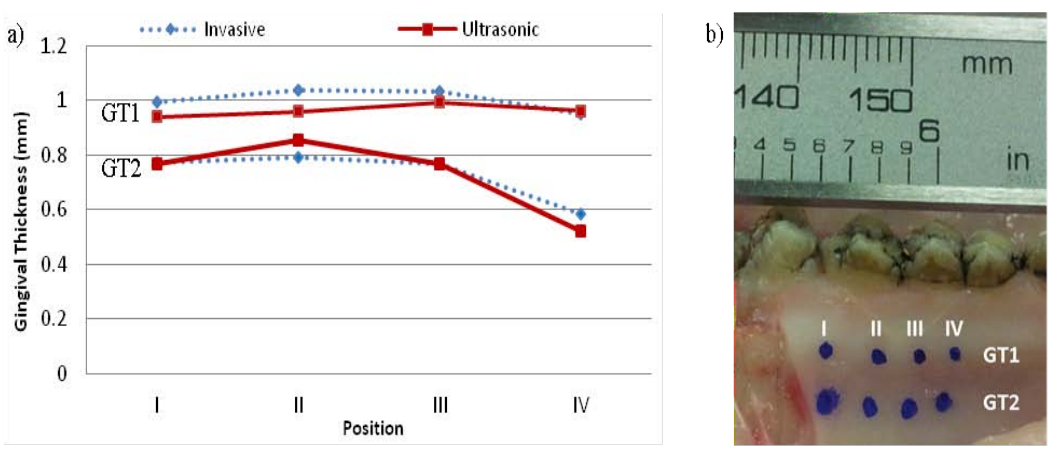

Figure 4.15 (a) GT1 and GT2 values from porcine cadaver; error for each datum is presented in table 4.4. (b) Eight measurement locations for porcine cadaver experiment.

Table 4.3 GT1 and GT2 results (in mm) for porcine cadaver. Values from the invasive method are presented with their associated reading error.

Position	I	II	III	IV	Method
GT1	0.99 ± 0.01	1.04 ± 0.01	1.03 ± 0.01	0.95 ± 0.01	Invasive
	0.94 ± 0.01	0.96 ± 0.09	0.99 ± 0.03	0.96 ± 0.03	Ultrasonic
GT2	0.77 ± 0.01	0.79 ± 0.01	0.77 ± 0.01	0.59 ± 0.01	Invasive
	0.77 ± 0.08	0.85 ± 0.03	0.77 ± 0.06	0.52 ± 0.01	Ultrasonic

Also, results obtained in the vertical line experiment were satisfactory. Three measurement techniques were used and the results are presented in figure 4.16. As a reference the gingival margin was assumed. The main influence for the errors calculated in these experiments had the geometry and difficulties with angle adjustments. Still the results are in close proximity and the bone edge could be easily detected due to thickness values change (it is highlighted by the discontinuity in graphs [Fig. 4.16]). Overall, gingival thickness from coronal to apical direction was assessed.

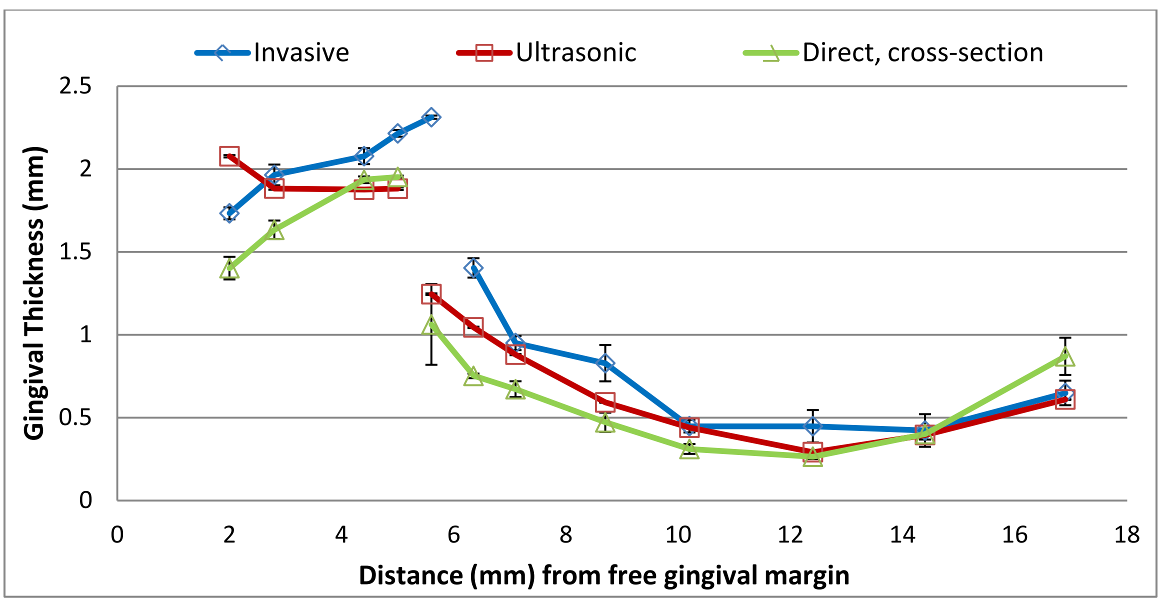

Figure 4.16 The bone crest detection experiment results.

4.3. Summary

The experimental results proved high potential of the ultrasonic technology to be used for intraoral measurements. In both experiments, tissue layers were successfully assessed and all ultrasonic results were compared to the ones obtained using the current gold-standard method or the cross-sectional direct measurement. Sources of possible difference exceeding the experimental error and variations associated with the experimental measurements will be discussed in the next chapter.

CHAPTER 5.

DISCUSSION

Ultrasonic measurements of the initial thickness of the enamel and its remaining thicknesses after consecutive grindings were found to be easy to implement by applying the UDS developed. Since the echo signal depended on the probe tip angle relative to the enamel surface, the probe was always aligned perpendicularly to the enamel surface by selecting the highest amplitude of the EDJ echo signals. The calculated axial resolution of 50 MHz transducer-based hand-held ultrasonic probe was 0.12 mm in the enamel.

Reproducibility (precision) and accuracy are important aspects of any measurement and diagnostic systems. For that reason, both were tested on the UDS using an ultrasonic calibration block (Albuquerque Industrial, Forest Hills, New York, USA). The signal shape (time spread) was analyzed for the device accuracy estimation as well as multiple thickness readings from the block were obtained for repeatability test. The outcome of those tests resulted in negligible values in comparison to accuracy and precision introduced by the variation in object properties. In the ultrasonic measurement of the enamel layer thickness remaining after grinding, reproducibility establishes the axial resolution (minimal thickness change that can be measured) of the method. However, to achieve this resolution in a dental diagnostic procedure, a few limiting factors have to be taken into account. Firstly, it is difficult to repeatedly place the hand-held probe exactly in the same spot on the unmarked enamel surface of the sample. Secondly, there is a gradual increase in thickness of the enamel layer between the cervical and incisal margins of the tooth that can considerably distort the repeated measurements of the enamel thicknesses in case the probe is slightly displaced from the initial position. In addition, manipulation of the probe to achieve proper alignment relative to the enamel layer surface can result in slight displacement of the probe on the surface. Moreover, the accuracy of the hand-held probe in measuring actual enamel thickness is highly dependent upon the longitudinal ultrasound velocity in enamel. This velocity shows some natural differences between teeth and can also depend on the age of the patient, probably due to changes in the density of the enamel. Another particular characteristic of the dental enamel is its anisotropy for sound propagation due to the specific arrangement of the hydroxyapatite crystalline rods. Such hydroxyapatite rods are found in rows along the tooth, and within each row, the long axis of the enamel rod is generally perpendicular to the underlying dentin, which usually results in different values of ultrasound velocity for longitudinal and transversal enamel sections. Therefore, the direct measurement of the velocity of sound in enamel remains the current technique of choice. As was shown in the present study, the longitudinal ultrasound velocity was calculated by determining the time delay between the echoes received from the surface of the sample and the enamel-dentin interface, and directly measuring the thickness of the enamel with the optical microscope from a cross-sectional view. The average velocity of 6100 ± 120 m/s is on the high end of the range reported in previous publications [4], [10], [95]. This could be due to the fact that measurements were all carried out essentially parallel to the rod direction and, therefore, a relatively high ultrasound velocity was to be expected. The accuracy of the measurements conducted is also considerably dependent on the shape of the reflected signal. Thus, the focal distance should be adjusted to locate the focal spot in close proximity to the enamel-dentine interface. Another important component of the measurement accuracy is the technique by which the reference points defining the time delay between the reflected signals were determined. A signal processing algorithm was developed for this purpose.

Results obtained in the hard dental tissue thickness measurement experiment validated the application of ultrasound for this purpose.

In the second part of the experimental work the gingival biotype was the objective of the study. The speed of sound used, to determine GT is often assumed to be equal to that through soft tissue [33], and typically falls within the range of 1514 – 1540 m/s [4], [33], [47], [79], [96]. The value of 1564 ± 21 m/s obtained in this experiment lies slightly higher. This could be due to the keratinization of gingival tissue which makes it more rigid than many other soft tissues. Error in the value determined for speed of sound was the result of anisotropy and heterogeneity throughout the tissue sample. Due to these phenomena TOF was not constant along the tissue, as was revealed by the speckle in the B-scan [Fig. 4.14]. For the speed of sound determination, averages of TOF across each medium were taken along with the standard deviation.

While assessing porcine GT, the invasive technique was implemented once at each location to mimic the *in vivo* standard diagnostic procedure [28], [83]. Error presented for this technique is reading error resulting from probing each location once and measuring displacement of the rubber limiter ten times with computer software. Conversely, error presented for the ultrasonic technique is generally greater in value since this error arose from taking ten separate measurements at each location (statistical calculation). It was found that average ultrasonic values were similar to invasive; GT1 measurements were greater than GT2, which has been found by a previous group studying human periodontium [28] which is shown by anatomy.

A k-file endodontic tool was used rather than a needle to avoid bending the needle during transgingival probing, since this would have resulted in overestimation of GT. Deviation in the invasive method could have arisen from inconsistency of the angle to the gingival surface at which the k-file needle was poked, or from movement of the rubber limiter along the needle upon removal from the mouth. Conversely, the needle may have been too thick to reach the bone surface, which would have resulted in an underestimation of the true value. Efforts were made to minimize reading error associated with invasive measurements by measuring displacement of the rubber limiter along the needle with computer software, as opposed to measuring with calipers [79]. However, in many cases, assessing the depth to which the needle penetrated gingival tissue was difficult when the limiter did not sit perpendicularly to the needle. This could have occurred in locations where the gingival surface and the bone were unparallel, or if one half of the limiter adhered to the gingival surface upon removal of the needle from the tissue. In addition, liquid residue on the front side of the needle made measuring precise displacement a challenge [Fig. 5.1].

Figure 5.1 The rubber limiter is shown adjacent to the thickness reference block (1.52 mm). Accurate GT assessment was made difficult when the limiter lay at an angle to the needle. Note the liquid residue at the tip of the needle, circled in red.

Specifically relating to the porcine cadaver experiment, GT1 was found to be greater in positions I, II and III by the invasive method than the ultrasonic method. It is possible that the second ultrasonic echo was received from the periosteum which covers the alveolar bone, while during invasive measurements the needle would have punctured through the periosteum and hit the bone. Deviation in the ultrasonic method arose from inconsistent positioning of the probe tip over a designated location during sequential trials. This experimental error yielded greater significance than the reading error associated with the ultrasonic technique.

The results of this experiment showed that ultrasound can yield accurate, quantitative data for the assessment of periodontal biotype. In addition to the discomfort, requirement for anesthesia, and risk of introducing infection, the measurement errors presented by the invasive technique of transgingival probing signify the need for a novel diagnostic approach. Further research will be done to optimize system performance. Future prospects include *in vivo* trials on human subjects, as well as the possible use of a multi-element ultrasonic transducer.

CHAPTER 6.

SUMMARY

A general outline to ultrasound in the medical field with a description of ultrasonic systems and a set of system requirements for the potential application in dentistry was described. The most popular dental diagnostic modalities were briefly reviewed and compared with the suggested ultrasonic solution. The introductory chapter is followed by insights to ultrasonic wave propagation to provide necessary knowledge required for device development, especially the transducer design. Next, the technical blocks of the proposed dental diagnostic system were described in details along with necessary parameters. The dental system was designed and assembled, and initially tested on prepared dental phantoms. Finally, two sets of experimental trials on hard and soft porcine dental tissues were conducted.

The HF ultrasound technology has shown the potential for detailed delineation of anatomical dental structures. In both experiments, tissue layers were successfully assessed and all ultrasonic results were compared to the ones obtained using the current gold standard method or the cross-sectional direct measurement.

REFERENCES/BIBLIOGRAPHY

[1] S. L. Oh, "Attached Gingiva: Histology and Surgical Augmentatation," *General Dentistry,* vol. 57, no. 4, pp. 381-385, 2009.

[2] S. Habalitz, S. J. Marshall, G. W. Marshall and M. Balooch, "Mechanical Properties of Human Dental Enamel on The Nanometer Scale," *Archives of Oral Biology,* vol. 46, no. 2, pp. 173-183, 2001.

[3] M. Hannig and C. Gannig, "Nanomaterials in Preventive Dentistry," *Nature Nanotechnology,* vol. 5, p. 565–569, 2010.

[4] R. G. Maev, Acoustic Microscopy, Weinheim: Wiley-VCH Verlag GmbH &Co. KGaA, 2008.

[5] J. H. Kinney, S. J. Marshall and G. W. Marshall, "The Mechanical Properties of Human Dentin: A Critical Review and Re-Evaluation for Dental Literature," *Critical Reviews in Oral Biology & Medicine,* vol. 14, no. 1, pp. 13-29, 2003.

[6] M. L. Listgarten, "Histology of the Periodontium," Univeristy of Pennsylvania and Taple University, 8 5 1999. [Online]. Available: http://www.dental.pitt.edu/informatics/periohistology/en/guin01m.htm.

[7] S. Lees and F. R. Rollins, "Anisotropy in Hard Dental Tissues," *Journal of Biomechanics,* vol. 5, no. 6, pp. 557-564, 1972.

[8] C. John, "The Corono-Apically Varying Ultrasonic Velocity in Human Hard Dental Tissues," *Journal of the American Society of America,* vol. 116, no. 1, pp. 544-556, 2004.

[9] H. Gawda, L. Sekowski and H. Trebacz, "In Vitro Examination of Human Teeth Using Ultrasound and X-ray Diffraction," *Acta of Bioengineering and Biomechanics,* vol. 6, no. 1, pp. 41-49, 2004.

[10] R. G. Maev, L. Denisova, E. Maeva and A. Denissov, "New Data On Histology and Physico-mechanical Properties of Human Tooth Tissue Obtained with Acoustic Microscopy," *Ultrasound in Medicine & Biology,* vol. 28, no. 1, pp. 131-136, 2002.

[11] L. Denisova, R. Maev, F. Rusanov, A. Maeva, A. Denisov, D. D. Y. Gavrilov, E. Y. Bakulin and F. M. Severin, "Fundamental Potential for Acoustic Microscopy in Evaluation of Dental Tissues," in *Acoustical Imaging*, San Diego, 2007.

[12] S. R. Ghorayeb, C. A. Bertoncini and M. K. Hinders, "Ultrassonography in Dentistry," *IEEE Transactions on Ultrasonics, Ferrolectrics and Frequency Control,* vol. 55, no. 6, pp. 1256-1266, 2008.

[13] G. Baum, I. Greenwood, S. Slawski and R. Smirnow, "Observation of Internal Structures of Teeth by Ultrasonography," *Science,* vol. 139, no. 3554, pp. 495-496, 8 February 1963.

[14] F. Barber, S. Lees and R. Lobene, "Ultrasonic Pulse-Echo Measurements in Teeth," *Archives of Oral Biology,* vol. 14, no. 7, pp. 745-760, July 1969.

[15] U. Keller, "High Frequency Sonography in Periodontal Diagnosis," *Dutsch Zahnärztl Zeitung,* vol. 44, no. 7, pp. 507-509, 1989.

[16] K. Ohshima, "Application of Ultrasonography to Periodontal Diagnosis," *Nippon Shishubyo Gakkai Kaishi,* vol. 31, pp. 235-240, 1989.

[17] K. S. Oikarinen, T. M. Nieminen, H. Makarainen and J. Pyhtinen, "Visibility of Foregin Bodies in Soft Tissue in Plain Radiographs, Computed Tomogrphy, Magnetic Resonance Imaging, and Ultrasound," *Internatinal Journal of Oral Maxillofeacial Surgries,* vol. 22, pp. 119-124, 1993.

[18] J. I. Kushibiki, L. K. Ha, H. Nato, N. Chubachi and F. Dunn, "Application of Acoustic Microsocpy to Dental Material Characterisation," in *IEEE Ultrasonics Symposium*, Denver, 1987.

[19] S. D. Peck and G. A. D. Briggs, "The Caries Lesion Under The Scanning Acoustic Microscope," *Advanced Denatal Research,* vol. 1, no. 1, pp. 50-63, 1987.

[20] I. Low and A. Alhuthali, "In-situ Monitoring of Dental Erosion in Tooth Enamel When Exposed To Soft Drinks," *Materials Science and Engineering,* pp. 1322-1325, 2008.

[21] J. Hua, S.-K. Chen and Y. Kim, "Refining Enamel Thickness Measurements From B-mode Ultrasound Images," in *31st Annual International Conference of the IEEE EMBS*, Minneapolis, 2009.

[22] F. O. Bozkurt, D. A. Tagtekin, O. Hayran, G. K. Stookey and F. C. Yanikoglu, "Accuracy of Ultrasound Measurment of Progressive Change in Occlusal Enamel Thickness," *Oral Surgery, Oral Medicine, Oral Pathology, Oral Radiology, and Endodontolgy,* vol. 99, no. 1, pp. 101-105, 2005.

[23] M. Huysmans and J. Thijssen, "Ultrasonic Measurement of Enamel Thickness: A Tool for Monitoring Dental Erosion?," *Journal of Dentistry,* vol. 28, pp. 187-191, 2000.

[24] C. Louwerse, M. Kjaeldgaard and M. Huysmans, "The Reproducibility of Ultrasonic Enamel Thickness Measurements: An In Vitro Study," *Journal of Dentistry,* vol. 32, pp. 83-89, 2004.

[25] B. Slak, A. Ambroziak, E. Strumban and R. G. Maev, "Enamel Thickness Measurement With a High Frequency Ultrasonic Transducer-Based Hand-Held Probe for Potential Application in The Dental Veneer Placing Procedure," *Acta of Bioengineering and Biomechanics,* vol. 13, no. 1, pp. 65-70, 2011.

[26] E. A. Aydrin and I. Guler, "Design of Pic-Controlled Pulsed Ultrasonic Transmitter for Measuring Gingiva Thickness," *Instrumentation Science and Technology,* vol. 38, pp. 411-420, 2010.

[27] H. P. Muller, N. Schaller and T. Eger, "Ultrasonic Determination of Thickness of Masticatory Mucosa," *Oral Surgery Oral Medicine Oral Pathology,* vol. 88, no. 2, pp. 248-253, 1999.

[28] W. Bednarz and A. Zielinska, "Ultrasonic Biometer and its Usage in an Assessment of Periodontal Soft Tissue Thickness and Comparison of its Measurement Accuracy with a Bone Sounding Method," *Journal of Dental and Medical Problems,* vol. 48, no. 4, pp. 481-489, 2011.

[29] W. Bednarz, "The Thickness of Periodontal Soft Tissue Ultrasonic Examination - Current Possibilities and Perspectives," *Journal of Dental Medical Problems,* vol. 48, no. 3, pp. 303-310, 2011.

[30] S. Harput, T. Evans, N. Bubb and S. Freear, "Diagnostic Ultrasound Tooth Imaging Using Fractional Fourier Transform," *IEEE Transactions on Ultrasonics, Ferroelectrics, and Frequency Control,* vol. 58, no. 10, pp. 2096-2106, 2011.

[31] S. Dos Santos and Prevorovsky, "Imaging of Human Tooth Using Ultrasonic Based Chirp-Coded Nonlinear Time Reversal Acoustics," *Ultrasonic,* vol. 51, no. 6, pp. 667-674, 2011.

[32] F. I. Tsiolis, I. G. Needleman and G. S. Griffiths, "Periodontal Ultrasonography," *Journal of Clinical Periodontology,* vol. 30, pp. 849-854, 2003.

[33] B. Salmon and D. Le Denmat, "Intraoral Ultrasonography: Development of a Specific High-frequency Probe and Clinical Pilot Study," *Clinical Oral Investigations,* vol. 16, no. 2, pp. 643-649, 2011.

[34] R. Chifor, E. M. Badea, M. Hedesiu, A. Serbanescu and F. A. Badea, "Experimental Model for Measuring and Characterisation of The Dento-Alveolar System Using High Frequencies Ultrasound Techniques," *Medical Ultrasonography,* vol. 12, no. 2, pp. 127-132, 2010.

[35] D. Huges, J. Girkin, S. Poland, C. Longbottom, T. Button, J. Elgoyhen, H. Hughes, C. Meggs and S. Cochran, "Inverstigation of Dental Samples Using a 35 MHz Focussed Ultrasound Piezocomposite Transducer," *Ultrasonics,* vol. 49, pp. 212-218, 2009.

[36] M. O. Culjat, M. Choi, R. S. Singh, W. S. Grundfest, E. R. Brown and S. N. White, "Ultrasound Detection of Submerged Dental Implants Through Soft Tissue in a Porcine Model," *The Journal of Prosthetic Dentistry,* vol. 99, pp. 218-224, 2008.

[37] D. A. Hughes, T. W. Button, S. Cochran, J. Elgoyhen, J. M. Girkin, H. Hughes, C. Longbottom, C. Meggs and S. Poland, "3D Imaging of Teeth Using High Frequency Ultrasound," in *IEEE Ultrasonic Symposium*, New York, 2007.

[38] C. John, "The Laterally Varying Ultrasonic Velocity in The Dentin of Human Teeth," *Journal of Biomechanics,* vol. 39, pp. 2388-2396, 2006.

[39] C. John, "Directing Ultrasound at The Cemento-Enamel Junction (CEJ) of Human Teeth: Asymmetry of Ultrasonic Path Lengths," *Ultrasonics,* vol. 43, pp. 467-479, 2005.

[40] L. Denisova, R. Maev, I. Poyurovskaya, T. Grineva, A. Denisov, E. Maeva and E. Bakulin, "The Use of Acoustic Microscopy to Study The Mechanical Properties of Glass-inomer Cement," *Journal of Dental Materials,* vol. 20, pp. 358-363, 2004.

[41] Y. Zheng, E. Maeva, A. Denisov and R. Maev, "Ultrasound Imaging of Human Teeth Using a Desktop Scanning Acoustic Microscope," *Acoustical Imaging,* vol. 24, pp. 165-170, 2000.

[42] E. Bakulin, L. Denisova and R. Maev, "A Study of The Potential to Detect Caries Lesions at The White-Spot Stage Using V(z) Technique," *Acoustical Imaging,* pp. 193-199, 2008.

[43] "American Dental Association," 2004. [Online]. Available: http://www.ada.org/sections/educationAndCareers/pdfs/dental_history.pdf.

[44] B. Vandenberghe, R. Jacobs and H. Bosmans, "Modern Dental Imaging: A Review of The Current Technology and Clinical Appilcaitons in Dental Practise," *Journal of Europian Radiology,* vol. 20, pp. 2637-2655, 2010.

[45] D. A. Tyndall and S. Rathore, "Cone-Beam CT Diagnostic Applications: Caries, Periodontal Bone Assessment, and Endodontic Applications," *Journal of Dental Clinics of North America,* vol. 52, no. 4, pp. 821-841, 2008.

[46] Y.-S. Hsieh, Y.-C. Ho, S.-Y. Lee, C.-C. Chunag, J.-c. Tsai, K.-F. Lin and C.-W. Sun, "Dental Optical Coherence Tomography," *Sensors ,* vol. 13, no. 1, pp. 8928-8949, 2013.

[47] H. Muller, N. Schaller, T. Eger and A. Heinecke, "Thickness of Masticatory Mucosa," *Journal*

oc Clinical Periodontology, vol. 27, no. 2, pp. 431-436, 2000.

[48] T. Terakura, "Non-Invasive Measurement of The Thickness of Oral Soft Tissues," *Journal of Japan Prosthodontics Society,* vol. 30, pp. 1402-1411, 1986.

[49] H. Uchida, K. Kobayashi and M. Nagao, "Measurement In Vivo of Masticatory Mucosal Thickness With 20 MHz B-mode Ultrasonic Diagnostic Equipment," *Journal of Dental Research,* vol. 68, no. 2, pp. 95-100, 1989.

[50] D. N. Cheeke, Fundamentals and Applications of Ultrasonic Waves, New York: CRC Press, 2002.

[51] L. W. Schmerr, Fundamentals of Ultrasonic Nondestructive Evaluation. A Modeling Approach, New York: Plenum Press, 1998.

[52] M. F. Insana, "Sound Attenuation in Tissue," in *Medical CT and Ultrasound: Current Technology and Applications* , Connecticut, American Association of Physicists in Medicine , 1995, pp. 19-33.

[53] F. A. Duck, A. C. Bake and H. C. Starritt, "Ultrasonic Properties of Tissues," in *Ultrasound in Medicine* , Bristol and Philadelphia , Institute of Physics Publishing , 1998, pp. 57-83.

[54] L. W. Schmerr and S. J. Song, Ultrasonic Nondestructive Evaluation Systems: Models and Measurements, New York : Springer Science , 2007.

[55] A. Penttinen and M. Luukkala, "The Impulse Response and Pressure Nearfield of a Curved Ultrasonic Radiator," *Journal of Physics D: Applied Physics,* vol. 9, no. 10, pp. 1547-1557, 1976.

[56] K. Snook, J. Z. Zhao and C. Alves, "Design, Fabrication and Evaluation of High Frequency, Single-Element Transducers Incorporating Different Materials," *IEEE Transacion on Ultrasoncs, Ferroelectrics and Frequency Control,* vol. 49, no. 2, pp. 169-176, 2002.

[57] M. O. Culjat, Development of an Ultrasound Imaging System for The Detecion of Subsurface Fractures and Caries in Human Teeth, Los Angeles: University of California, 2005.

[58] Q. Zhou, S. Lau, D. Wu and K. K. Shung, "Piezoelectric Films for High Frequnecy Ultrasonic Transducers in Biomedical Applicanions," *Progress in Materials Science,* vol. 56, no. 2, pp. 139-174, 2011.

[59] N. Instruments, "National Instruments," National Instruments, 02 10 2012. [Online]. Available: http://www.ni.com/white-paper/5369/en/.

[60] T. Kondo and M. Kitatiju, "New Tissue Mimicking Materials for Ultrasound Phantoms," in *IEEE Ultrasonics Symposium*, 2005.

[61] A. Wydra, E. Malyarenko, K. Shapoori and R. Maev, "Development of a Practical Ultrasonic Approach for Simultaneous Measurement of The Thickness and the Sound Speed in Human Skull Bones: A Laboratory Phantom Study," *Physics in Medicine and Biology,* vol. 58, no. 4, pp. 1083-1102, 2013.

[62] G. Christensen, "What is Veneer? Resolving The Confusion," *Journal of the American Dental Association,* vol. 135, no. 1, pp. 1574-1576, 2004.

[63] A. Ivoclar Vivadent, "Technical Notes:IPS w.max CAD, Instructions for Use," Lichtenstein, 2009.

[64] "American Dental Association Specification No. 8," *Journal of the American Dental Association,* vol. 57, pp. 121-123, 1978.

[65] M. Peumans, B. Van Meerbeek, P. Lambrecgts and G. Vanherle, "Porcelain Veneers: A Review of The Literature," *Journal of Dentistry,* vol. 28, no. 3, pp. 163-177, 2000.

[66] M. Piemjai and M. Arksornnukit, "Compressive Fracture Resistance of Porcelain Laminates Bonded to Enamel or Dentin with Four Adhesive Systems," *Journal of Prosthodontics,* vol. 16, no. 6, pp. 457-464, 2007.

[67] B. Smith and J. Knight, "An Index for Measuring The Wear of Teeth," *British Dental Journal,* vol. 256, pp. 649-653, 1984.

[68] S. Hooper, N. Meredith and D. Jagger, "The Development of a New Index for Measurement of Incisal/Oclusal Tooth Wear.," *Journal of Oral Rehabilitation,* vol. 31, pp. 206-212, 2004.

[69] S. Toda, T. Fujita, A. Arakwa and K. Toda, "An Ultrasonic Nondestructive Technique for Evaluating Layer Thickness in Human Teeth," *Sensors and Actuators A: Physical,* vol. 125, pp. 1-9, 2005.

[70] M. Culjat, R. Singh, D. Yoon and E. Brown, "Imaging of Human Tooth Enamel Using Ultrasound," *IEEE Transactions on Medical Imaging,* vol. 22, no. 4, pp. 526-529, 2003.

[71] S. Ng, P. Payne, N. Cartledge and M. Ferguson, "Determination of Ultrasonic Velocity in Human Enamel and Dentine," *Archives of Oral Biology,* vol. 34, no. 5, pp. 341-345, 1989.

[72] J. Kushibiki, K. Ha, H. Kato and N. Chubachi, "Application of Acoustic Microscopy to Dental Material Characterization," *IEEE 1987 Ultrasonics Symposium,* pp. 837-842, 1987.

[73] L. A. Denisova, R. G. Maev, F. S. Rusanov, A. R. Maeva, A. F. Denisov, D. Y. Gavrilov, E. Y. Bakulin and F. M. Severin, "Fundamental Potential for Acoustic Microsocpy Evaluation of Dental Tissues," in *Acoustical Imaging*, San Diego, 2007.

[74] J. Brucia, "Adhesive Dentistry: Materials & Techniques Simplified," San Francisco , 2005.

[75] R. Kao and K. Pasquinelli, "Thick vs. Thin Gingval Tissue : A Key Determienat in Tissue Response to Disease and Restorative Treatment," *Journal of the California Dental Association,* vol. 30, no. 7, pp. 521-526, 2002.

[76] M. Cuny-Houchmand, S. Renaudin, M. Leroul, L. Planche, L. Guehennec and A. Soueidan, "Gingival Biotype Assessment: Visual Inspection Relevance and Maxillary Versus Mandibular," *The Open Dentistry Journal,* vol. 7, pp. 1-6, 2013.

[77] H. Grover, A. Yadav, P. Yadav and P. Nanda, "Optimizing Gingival Biotype Using Subepithelial Connective Tissue Graft: A Case Report and One-Year," Hindawi Publishing Corporation, Gurgaon, India, 2011.

[78] R. Kao, M. Fagan and G. Conte, "Thick vs. Thin Gingival Biotypes: A Key Determinant in Treatment Planning for Dental Implants," *Journal of the California Dental Association,* vol. 36, no. 3, pp. 193-198, 2008.

[79] W. Bednarz, "The Thickness of Periodontal Soft Tissue Ultrasonic Examination: Current Possibilities and Perspectives," *Dental Medical Problems,* vol. 48, pp. 303-310, 2011.

[80] L. Huang, R. Neiva and H. Wang, "Factors Affecting The Outcomes of Coronally Advanced Flap Root Coverage Procedure," *Journal of Periodontolgy,* vol. 76, no. 10, pp. 1729-1734, 2005.

[81] D. Hwang and H. Wang, "Flap Thickness as a Predictor of Root Coverage: A Systematic Review," *Journal of Periodontology,* vol. 77, no. 10, pp. 1625-1634, 2006.

[82] J. Ackerman and W. Proffit, "Soft Tissue Limitations in Orthodontics: Treatment Planning Guidelines," *The Angle Orthodontist,* vol. 67, no. 5, pp. 327-336, 1997.

[83] B. Savitha and K. Vandana, "Comparative Assesment of Gingival Thickness Using Transgingival Probing and Ultrasonographic Method," *Indian Juornal of Dental Research,* vol. 16, no. 4, pp. 135-169, 2005.

[84] T. De Rouck, R. Eghbali, K. Collys, H. De Bruyn and J. Cosyn, "The Gingival Biotype Revisited: Transparency of The Periodontal Probe Through the Gingival Margin as a Method to Discriminate Thin From Thick Gingiva," *Journal of Clinical Periodontology,* vol.

36, no. 5, pp. 428-433, 2009.

[85] J. Kan, T. Morimoto, K. Rungcharassaeng, P. Roe and D. Smith, "Gingival Biotype Assessment in The Esthetic Zone: Visual Versus Direct Measurement," *The International Journal of Periodontics & Restorative Dentistry,* vol. 30, no. 3, pp. 237-243, 2010.

[86] R. Da Silva, J. Joly, A. De Lima and D. Tatakis, "Root Coverage Using The Coronally Positioned Flap With or Without a Subepithelial Connective Tissue Graft," *Journal of Clinical Periodontology,* vol. 75, no. 3, pp. 413-419, 2004.

[87] M. Barriviera, W. Duarte, A. Januario, J. Faber and A. Bezerra, "A New Method To Assess and Measure Palatal Masticatory Mucosa by Cone-beam Computerized Tomography," *Journal of Clinincal Periodontology,* vol. 36, no. 7, pp. 564-568, 2009.

[88] M. Si, L. Zhuang, X. Huang, Y. Gu, C. Chou and H. Lai, "Papillae Ilterations Around Single-Implant Restorations in the Anterior Maxillea: Thick Versus Thin Mucosa," *International Journal of Oral Science,* vol. 4, no. 2, pp. 94-100, 2012.

[89] A. Geiger, "Mucogingival Problems and The Movement of Mandibular Incisors: A Clinical Review," *Amemrican Journal of Orthodontics,* vol. 78, no. 5, pp. 511-527, 1980.

[90] M. Olsson and J. Lindhe, "Periodontal Characteristics in Individuals with Varying Form of The Upper Central Incisors," *Journal of Clinical Periodontology,* vol. 18, no. 1, pp. 78-82, 1991.

[91] D. Cook, B. Mealey, R. Verrett, M. Mills, M. Noujeim, D. Lasho and R. Cronin, "Relationship Between Clinical Periodontal Biotype and Labial Plate Thickness: An In Vivo Study," *The Internetional Journal of Periodontics & Restorative Dentistry,* vol. 31, no. 4, pp. 345-354, 2011.

[92] C. Dahlin, M. Simion and N. Hatano, "Long-Term Follow-Up on Soft and Hard Tissue Levels Following Guided Bone Regeneration Treatment in Combination with a Xenogeneic Filling Material: A 5-Year Prospective Clinical Study," *Clinical Implant Dentistry and Related Research,* vol. 12, no. 4, pp. 263-270, 2010.

[93] R. Davies, M. Downer, P. Hull and M. Lennon, "Alveolar Defects in Human Skulls," *Journal of Clinical Periodontology,* vol. 1, no. 2, pp. 107-111, 1974.

[94] A. Briggs, Acoustic Microscopy, Oxford : Clarendon Press, 1992.

[95] L. Denisova, R. Maev, V. Leontjev, A. Denisov, G. Grayson, F. Rusanov, E. Bakulin, D. Gavrilov and T. Grineva, "A Study of The Adhesion Between Dental Cement and Dentin Using a Nondestructive Acoustic Microscopy Approach," *Dental Materials ,* vol. 25, pp.

557-565, 2009.

[96] R. Schulze, D. Curic and B. D'Hoedt, "B-mode Versus A-mode Ultrasonographic Measurements of Mucosal Thickness In Vivo," *Oral Surg Oral Med Oral Patho,* vol. 93, pp. 110-117, 2002.

APPENDICES

Appendix A

```
%BartoszSlak@IDIR

clear all
clc
density1=1000;
density2=2970;
velocity_1=1480;
velocity_L2=5900;
velocity_S2=3200;
teta_L=0;

for i=1:6000
    if real(teta_L)<85
        teta_in=i/100;
        teta_L=(asind((velocity_L2*(sind(teta_in)))/velocity_1));
        teta_S=((asind((velocity_S2*(sind(teta_in)))/velocity_1)));
        Z_L=(density2*velocity_L2)/(cosd(teta_L));
        Z_S=(density2*velocity_S2)/(cosd(teta_S));
        Z_1=(density1*velocity_1)/(cosd(teta_in));
        down=((Z_L*((cosd(2*teta_S))^2))+(Z_S*(sind(2*teta_S))^2)+Z_1);
        down1=((Z_L*((cosd(2*teta_S))^2))+(Z_S*(sind(2*teta_S))^2)-
Z_1);
        up=2*Z_L*cosd(2*teta_S);
        up_shear=2*Z_S*sind(2*teta_S);
        front=(density2*tand(teta_in))/(density1*tand(teta_L));
        front_shear=(density2*tand(teta_in))/(density1*tand(teta_S));

trans_long(i)=(front*(abs((density1/density2)*(up/down)))^2)*100;
        reflection(i)=((abs(down1/down))^2)*100;
        trans_shear(i)=(front_shear*(abs((-
density1/density2)*(up_shear/down)))^2)*100;

    end
end

 figure()
 plot((1:(length(trans_long)))/100,trans_long)
 hold on
 plot((1:(length(trans_shear)))/100,trans_shear,'red')
 plot((1:(length(reflection)))/100,reflection,'black')
 axis([0 14.5 0 100])
  h = legend('T_L','T_S','R',3);
set(h,'Interpreter','none')
 title('Water/Enamel angular depnedences on coeff')
 xlabel('Incidence angle [deg]')
 ylabel('Energy [%]')
```

VITA AUCTORIS

NAME:	Bartosz Slak
PLACE OF BIRTH:	Sycow, Lower Silesia, Poland
YEAR OF BIRTH:	1985
EDUCATION:	University of Technology in Wroclaw, Faculty of Fundamental Problems of Technology, Department of Technical Physics, B.Sc. & M.Sc. combined program, Wroclaw, Lower Silesia, Poland, 2009